This is the accepted manuscript version of the contribution published as:

Saeidi, N., **Kopinke, F.-D.**, **Georgi, A.** (2021):
What is specific in adsorption of perfluoroalkyl acids on carbon materials?
Chemosphere **273** , art. 128520

The publisher's version is available at:

http://dx.doi.org/10.1016/j.chemosphere.2020.128520

What is specific in adsorption of perfluoroalkyl acids on carbon materials?

Navid Saeidi, Frank-Dieter Kopinke, Anett Georgi *

Helmholtz Centre for Environmental Research – UFZ, Department of Environmental Engineering, D-04318 Leipzig, Germany

Corresponding author contact information: Tel.: +49 341 235 1760; Fax: +49 341 235 1471; E-mail: anett.georgi@ufz.de

Abstract

Various activated carbon products show wide variability in adsorption performance towards perfluoroalkyl acids (PFAAs) and predictive tools are largely missing. In order to gain a better understanding on the adsorption mechanisms of PFAAs, perfluorooctanoic acid (PFOA) was compared with its fluorine-free analogon octanoic acid (OCA) as well as phenanthrene (nonionic) in terms of their response towards changes in carbon surface chemistry. For this approach, a commercial activated carbon felt (ACF) with high content of acidic surface groups was modified by amino-functionalisation as well as thermal defunctionalisation in H_2 (yielding DeCACF). While improvement by amino-functionalisation was moderate, defunctionalisation drastically enhanced adsorption of PFOA and other PFAAs. In comparison, OCA and phenanthrene were much less affected. Electrostatic interactions and charge compensation provided by positively charged surface sites (quantified by their anion exchange capacity) are obviously more crucial for PFAAs than for common organic acids (such as the tested OCA). A possible reason is their exceptionally strong acidity with $pK_a < 1$. Nevertheless, at the best modified ACF material (DeCACF) the sorption coefficients (K_d) for PFOA and perfluorooctylsulfonic acid (PFOS) at environmentally relevant concentrations reach the range of 10^7 L/kg which is outstanding. DeCACF provides a surface with overall low polarity (low O-content), low density of acidic sites causing electrostatic repulsion, but nevertheless a sufficient density of charge-balancing sites for organic anions. The results of the present study contribute to an optimised selection of adsorbents for PFAA adsorption from water considering also various salt matrices and the presence of natural organic matter.

Keywords:

PFOA; PFOS; PFBA; Octanoic acid; Activated carbon; Adsorption mechanism.

Nomenclature

AC	activated carbon
ACF	activated carbon felt
AEC	anion exchange capacity
CACF	commercial activated carbon felt
$CACFNH_2$	amino-functionalised activated carbon felt
C_0	initial concentration of solute in solution
C_e	equilibrium concentration of solute in solution
CEC	cation exchange capacity
DeCACF	defunctionalised activated carbon felt
K_F	Freundlich adsorption coefficient
K_L	Langmuir adsorption coefficient
K_d	single-point adsorption coefficient
K_{ow}	octanol-water partitioning coefficient
m	mass of activated carbon felt
n	Freundlich exponent
NOM	natural organic matter
OCA	octanoic acid
PFAAs	perfluoroalkyl acids
PFBA	perfluorobutanoic acid
PFOA	perfluorooctanoic acid
PFOS	perfluorooctylsulfonic acid
PHE	phenanthrene
PSD	pore size distribution
PZC	point of zero net proton charge
pK_a	negative logarithm of the acid dissociation constant
q_e	equilibrium concentration of adsorbed solute on adsorbent
q_m	Langmuir maximum adsorption capacity of adsorbent
R^2	correlation coefficient
SRNOM	Suwannee River natural organic matter
t	time
TPD	temperature-programmed decomposition
V	volume of solution
V_p	pore volume
V_{total}	total pore volume
XPS	X-ray photoelectron spectroscopy

1. Introduction

Perfluoroalkyl acids (PFAAs) are a class of fully fluorinated hydrocarbons. In the last 60 years these compounds have been used for producing non-stick, waterproof and stain-resistant coatings for various products (Teaf et al., 2019). They are the focus of current attention because of their detection in various sources of water and a rapid increase in evidence for their adverse health effects, including tumour induction, hepatoxicity, developmental toxicity, immunotoxicity, endocrine disruption and neurotoxicity (Sznajder-Katarzyńska et al., 2019).

The compounds with eight carbon atoms, perfluorooctanoic acid (PFOA) and perfluorooctylsulfonic acid (PFOS), are the most studied PFAAs, although recent research has also revealed the occurrence of shorter-chain PFAAs in drinking water (Brendel et al., 2018; Phong Vo et al., 2020). PFOS (in 2009) and PFOA (in 2019) were added to Annex B of the Stockholm Convention on Persistent Organic Pollutants (Higgins and Field, 2017). Since June 2013, PFOA and its ammonium salt are considered as chemicals of "very high concern" by the European Chemicals Agency (T. Pancras, 2016). Thereafter, shorter-chain PFAAs and polyfluorinated compounds with smaller perfluoroalkyl structural elements have increasingly been developed as replacement compounds (Higgins and Field, 2017). Despite of some shorter-chain fluorinated alternatives being less bioaccumulative, these compounds or their perfluorinated degradation products are still persistent in the environment (Higgins and Field, 2017; Phong Vo et al., 2020). In addition, due to the lower efficiency of the shorter-chain PFAAs, larger amounts might be needed for obtaining the same performance (Brendel et al., 2018).

Remediation of sites with PFAAs soil and groundwater contamination is extremely challenging (Arias Espana et al., 2015; Gagliano et al., 2020). So far, there are no *in-situ* remediation technologies available. The most common treatment technology is pump-and-treat with subsequent treatment of the PFAAs contaminated water by adsorption onto activated carbon (AC) (Gagliano et al., 2020). However, there are some drawbacks which reduce the performance of PFAAs adsorption, i.e. highly variable removal efficiencies due to competitive adsorption by natural organic matter (NOM) (Rahman et al., 2014; Gagliano et al., 2020) and the use of shorter-chain PFAA replacement products such as perfluorobutanoic acid (PFBA) which has resulted in serious problems in water treatment (McCleaf et al., 2017). More importantly, although a number of studies have considered the mechanism of PFAAs adsorption on AC, some of the observed

phenomena still provoke questions. Adsorption affinities of PFOA and PFOS, for instance, can differ extremely between various AC products, i.e. by up to 4 orders of magnitude in sorption coefficients under the same experimental conditions (Deng et al., 2015; Zhi and Liu, 2016; Saeidi et al., 2020; Sörengård et al., 2020). To our knowledge, such huge differences in adsorption affinity on various ACs have rarely been observed for other organic compounds.

Understanding and prediction of sorption phenomena for organic compounds is of great importance in environmental science and engineering. For non-ionic organic compounds, polyparameter linear free energy relationships (PP-LFER) were successfully developed and applied for prediction of absorption and, with some limitations, even for adsorption equilibria (Endo and Goss, 2014). However, there is still a lack of prediction tools for sorption of ionic compounds (Endo and Goss, 2014; Sigmund et al., 2020). Sigmund et al. (Sigmund et al., 2020) have very recently reported a model to predict Freundlich isotherm parameters for adsorption of ionisable compounds to carbonaceous adsorbents using a deep learning neural network approach. However, PFAAs were not included in their training data set and the required molecule parameters for this compound class are not available. Improved mechanistic understanding and identification of decisive adsorbent properties is required as basis for development of predictive tools but also targeted adsorbent optimization.

We believe that a direct comparison of the adsorption behaviour of PFAAs and other model compounds, i.e. octanoic acid (OCA) and phenanthrene (PHE), for a set of well-characterised ACs can help to explain what is so special about adsorption of PFAAs on AC. OCA is the non-fluorinated structural analogue to PFOA. It has, however, a much weaker acid group (pK_a = 4.9 (Wellen et al., 2017)). PHE, as a neutral molecule, is a representative of the 3-ring

polycyclic aromatic hydrocarbons with high hydrophobicity (log $K_{OW, PHE}$ = 4.57 (Karickhoff, 1981)) and thus high adsorption affinity on AC (Walters and Luthy, 1984).

Furthermore, there is still discussion on what characteristic of AC can be considered as a good indicator of PFAAs' adsorption performance. Electrostatic interactions or anion exchange between protonated sites on ACs and anions of PFOA (pK_a between 0 and 1 (Goss, 2008)) and PFOS (pK_a = -3.27 (Brooke D., 2004)) have been considered as important contributions for adsorption of PFAAs (Zhi and Liu, 2015). In our previous work, we studied four commercial activated carbon felts (ACFs) and correlated the uptake of PFOA and PFOS by the adsorbents with various surface properties (Saeidi et al., 2020). Samples with low content of oxygen and high anion exchange capacity (AEC) provided excellent adsorption which was assigned to the interplay of hydrophobic and electrostatic interactions between PFAA anions and positively charged sites of the ACFs (Saeidi et al., 2020). Alternatively, point of zero net proton charge (PZC) has been addressed as an indicator for adsorption behaviour of various adsorbents towards PFAAs: the higher the PZC, the higher the sorption affinity (Du et al., 2014; Inyang and Dickenson, 2017; Hassan et al., 2020). Zhi and Liu (Zhi and Liu, 2015, 2016) have, however, reported that this hypothesis is not always true for uptake of PFOA and PFOS on AC. Thus, in this study we considered various parameters for description of surface properties of AC, including beside porosity and PZC also cation exchange capacity (CEC), AEC, O-content, N-content and content of various acidic groups. The set of AC used for these correlations builds upon as-received AC materials (data from our previous study, Saeidi et al., 2020) but is extended in this study by targeted modification for obtaining improved adsorption. These modifications were done with the rationale to further decrease the density of repulsive anionic and increase the number of charge-balancing cationic surface sites for PFAA anion adsorption while maintaining an overall rather non-polar

carbon surface. Thermal defunctionalisation to remove acidic oxygen-containing groups from AC and to increase the π-electron-based basicity (Shafeeyan et al., 2010) and amino-functionalisation to create net positive surface charge at near-neutral pH (Cai and Larese-Casanova, 2016; Zhang et al., 2016) were selected as modification strategies. Amino-functionalised sorbents, e.g. chitosan-based polymers (Long et al., 2019), poly(ethylenimine)-functionalised cellulose (Ateia et al., 2018) and amino-functionalised covalent organic framework (Ji et al., 2018), have recently emerged as novel materials with effective performance in PFAAs removal (Phong Vo et al., 2020). Amino-functionalised cellulose has shown promising potential for being an effective adsorbent for PFAAs in a wide range of pH (from 4.5 to its PZC=10.9) and in presence of competitive inorganic and organic compounds (Ateia et al., 2018). The authors suggested to also apply amino-functionalisation strategies for enhancing performance of other conventional adsorbents towards PFAAs.

To follow the above mentioned goals, a commercial microporous ACF (CACF) with comparably high content of acidic groups, was used for preparation of amino-functionalised ACF ($CACFNH_2$) and defunctionalised ACF (DeCACF). In particular, this work addresses the questions of what is specific in adsorption of PFAAs on carbon materials and which type of basic groups on the AC increases uptake of long-chain and short-chain PFAAs from water.

2. Materials and Methods

2.1. Materials

PFOA, PFOS and PFBA (96%, 98% and 98% purity, respectively) as well as PHE (98%) and octanoic-d_{15} acid were purchased from Sigma-Aldrich (USA). HCl (fuming 37%), NaOH, $NaHCO_3$, KCl, $NaNO_3$, $MgSO_4$, CH_3COONH_4, Na_2CO_3 and Na_2SO_4 (all in highest available purity) were obtained from Merck (Germany). Thionyl chloride (98% for synthesis),

ethylenediamine (99.5% for synthesis) and OCA (>99% for synthesis) were obtained from CARL ROTH (Germany). Tetrahydrofuran (THF) (pure) was purchased from Applichem (Germany). Methanol of HPLC grade was bought from Th. Geyer (Germany). Suwannee River natural organic matter (SRNOM, reference number: 2R101N) was obtained from International Humic Substances Society (IHSS).

2.2. Activated carbon felt

The ACF was provided by Jacobi CARBONS, Sweden. The commercial name of the ACF is ACTITEX WK L20 (CACF). The CACF was rinsed first with pure methanol and then deionized water before usage.

2.2.1. Amino-functionalisation and defunctionalisation of ACF

CACF was functionalised using ethylenediamine by a procedure reported elsewhere (Qiu et al., 2013; Zhang et al., 2016) with some alterations. Ethylenediamine is connected to the AC surface through an amide bond between one of its amine groups and a surface carboxyl group, whereby the other amine group is able to provide a positive surface charge (as $–NH_3^+$) when pH < pK_{a1} (Cai and Larese-Casanova, 2016). In our previous work, we determined the concentration of carboxylic groups of CACF by Boehm titration as 1.26 mmol/g or 1.12 µmol/m^2, which is quite high. Therefore, we used it as received without any modification for creating carboxylic groups on it. In brief, 150 mg of CACF was dried at 60°C overnight and then stirred in 30 mL of thionyl chloride ($SOCl_2$) at 75°C for 24 h. After the acyl chlorination (-COOH → -COCl), the ACF was washed with anhydrous THF five times and dried at 50°C for 1 h. The acyl-chlorinated CACF was reacted with 50 mL ethylenediamine at 100°C for 2 days. After cooling to room temperature, the amino-functionalised product ($-CONH-CH_2-CH_2-NH_2$, named $CACFNH_2$) was washed with

methanol five times and then with deionised water in order to remove excess diamine. Finally, the $CACFNH_2$ was dried at 50˚C overnight and kept in a desiccator for further use.

In addition, CACF was treated thermally under pure hydrogen in order to remove oxygen-containing groups from the ACF and saturate any active sites produced. The procedure reported in (Menéndez et al., 1996) was applied with some modifications. In brief, a certain amount of CACF was placed in a tube furnace, purged with nitrogen for 1 h and then with hydrogen for 30 min at ambient temperature, heated with a ramp of 50 K /min up to 900 ˚C and kept at 900 ˚C for 2 h. Finally, the sample cooled down to ambient temperature under a flow of hydrogen.

2.2.2. Characterisation of the activated carbon felts

The physical properties of the adsorbents, e.g. fiber diameter, specific surface area, pore volume and pore size distribution (PSD), were determined by procedures reported in detail in our previous work (Saeidi et al., 2020).

Characterisation of surface chemistry of the ACFs was done by determination of PZC, acidic surface functional groups by Boehm titration, AEC and CEC of the ACFs as well as temperature-programed decomposition (TPD) as also described in our previous work (Saeidi et al., 2020). X-ray photoelectron spectroscopy (XPS) was performed using an Axis Ultra photoelectron spectrometer (Kratos, Manchester, UK) using monochromatised Al Kα radiation ($h\nu$ = 1486.6 eV).

2.3. Analytical methods

Concentration of PFOA, PFOS, PFBA and OCA in solution was measured using a liquid chromatography system coupled to a single-stage quadrupole mass spectrometer with electrospray ionisation (LCMS-2020; Shimadzu, Japan). To analyse the concentration of the PFAAs in solutions, aliquots of 3 µL of the samples were injected into a 100 mm × 2 mm Gemini C6-Phenyl

column filled with fully porous organo-silica having 110 Å pore size and 3 µm particle size (Phenomenex, USA). A combination of solvent A, consisting of 5 mM ammonium acetate dissolved in 90% deionized water and 10% methanol, and solvent B, consisting of 5 mM ammonium acetate dissolved in 90% methanol and 10% water was used as mobile phase. The LC pump delivered a mix of solvent A (30%) and solvent B (70%) at a flow rate of 3 mL/min. The column temperature was kept at 40 ˚C during the run which was 10 min. For concentrations < 1 mg/L the correlation coefficients (R^2) of the calibration curves for the PFAAs were > 0.99 and the standard deviations for 5 measurements were around 5%. The detection limit for PFAAs were 0.05 µg/L.

Since the detection limit of the LCMS for OCA was around 100 µg/L, after adsorption experiments the solutions were concentrated by a factor of about 50 using Strata^{TM}-X cartridges (Phenomenex, USA). Octanoic-d_{15} acid was used as internal standard and added into the solutions before the preconcentration procedure. The correlation coefficients (R^2) of the calibration curves for OCA and octanoic-d_{15} acid for concentrations less than 3 mg/L were > 0.99.

PHE was analysed by means of HPLC with fluorescence detection (λ_{ex} = 244 nm, λ_{em} = 440 nm, Hewlett-Packard Series 1100, Agilent, Germany) using a Lichrospher 60 RP-C18 column (5 µm, Merck, Germany). The mobile phase consisted of acetonitrile/water (65:35) delivered at a flow rate of 0.5 mL/min (25 ˚C).

2.4. Adsorption experiments

Adsorption of the target compounds on the adsorbents was performed in 25 mL glass vessels. To simulate the ionic strength of tap water, 10 mM Na_2SO_4 was used as background electrolyte. In the case of OCA adsorption, 100 mL vessels filled with 100 mL electrolyte solution were used. The ACFs were weighted and added to the vessels. 0.1 M HCl or NaOH solutions were

used to provide the desired solution pH. After 24 h shaking, the pH of the suspensions was adjusted back to the desired values. Certain concentrations of the target solutes were then spiked from stock solutions. To study the effect of NOM on adsorption of the target solutes, 5 mg/L NOM was spiked from 100 mg/L NOM stock solutions.

The loading of the target adsorbates on the adsorbents was obtained as follows:

$$q_e = \frac{V \times (C_0 - C_e)}{m} \quad (1$$

here q_e (µmol/kg or µmol/m² if normalized by specific surface area of the adsorbent, as determined e.g. by BET analysis) denotes loading of adsorbate on the adsorbent at equilibrium. The initial concentration and concentration of adsorbate in solution at equilibrium are addressed by C_0 and C_e (µmol/L), respectively. V denotes the volume of solution in L and m is the mass of the adsorbent in kg.

The single-point adsorption coefficient K_d (L/kg or L/m²) of the solutes on the adsorbents can be calculated by Eq. (2):

$$K_d = \frac{q_e}{C_e} \quad (2$$

where the loading q_e is divided by the concentration of the solute in solution at equilibrium C_e. Equilibrium was considered to be approached after 2 d, as no significant changes in the aqueous phase solute concentrations were observed (≤ 5%) at further prolonged contact time.

2.4.1. Adsorption isotherms

Adsorption isotherms were obtained by fitting experimental data with a linearised form of the Langmuir equation (Eq. 3):

$$\frac{C_e}{q_e} = \frac{C_e}{q_m} + \frac{1}{q_m \times K_L} \quad (3$$

In Eq. 3, q_m (μmol/m^2) is the maximum monolayer loading of the adsorbate on the ACF and K_L (L/μmol) is the Langmuir constant which denotes the adsorption affinity of the solute on the adsorbent.

The data were also fitted with a linearised form of the empirical Freundlich equation (Eq. 4):

$$log\ q_e = n \times log\ C_e + log\ K_F \quad (4$$

In Eq. 4, K_F ((μmol/m^2)/(μmol/L)^n) is the Freundlich constant which denotes the adsorption affinity, while n is the Freundlich exponent (dimensionless).

3. Results and discussion

3.1. Properties of ACFs

Total pore volume (V_{total}), pore volume (V_p) in certain ranges of pore widths and fiber diameters of the ACFs are listed in Table 1. Figure 1S shows PSD of the ACFs. A detailed discussion on physical properties of the ACFs and the effect of surface modification of the ACFs on their PSDs can be found in Supporting Information.

Table 1. Physical properties of the investigated activated carbon felts.

Sample	BET surface area (m^2/g) [a]	V_{total} (cm^3/g) [a]	V_P in 1-2 nm pore width (cm^3/g) [b]	V_P in pore width < 1 nm (cm^3/g) [b]	Fiber Diameter (μm) [c]
CACF	1100	0.53	0.14	0.23	12 ± 1
CACFNH$_2$	720	0.30	0.084	0.13	12 ± 2
DeCACF	1000	0.46	0.16	0.15	6.5 ± 1

[a] obtained using N_2 adsorption/desorption, [b] obtained using CO_2 adsorption,
[c] an average of 10 measurements was reported.

The surface chemical properties of the ACFs are shown in Table 2. The ACFs differ significantly in their surface functional groups. CACF owns the highest concentrations of carboxylic (1.12 μmol/m^2) and total acidic groups (2.08 μmol/m^2) among the ACFs. Amino-functionalisation by amidation reduced the concentration of free carboxylic groups (causing negative charge at near-neutral pH) by about 45%. All types of acidic groups were affected by the thermal defunctionalisation, resulting in a decrease in total acidity and concentration of carboxylic groups by one order of magnitude.

Table 2. Chemical surface characteristics of the activated carbon felts.

Sample	Boehm titration				TPD					XPS	PZC
	pK_a ~ 3-6	pK_a ~ 6-10	pK_a ~ 10-13	pK_a ~ 3-13							
	Carboxylic acids	Lactones and lactols	Phenols	Total acidity	CO	CO_2	NH_3	O[a]	N[b]	N	
	μmol/m^2							wt%			
CACF	1.12	0.321	0.643	2.08	3.39	2.14	-	13.7	-	0.47	5.9 ± 0.2
$CACFNH_2$	0.611	0.264	0.710	1.58	3.33	1.66	1.0	7.90	1.1	2.6	7.3 ± 0.1
DeCACF	0.0233	0.130	0.0670	0.220	0.550	0.0840	-	1.10	-	0.33	9.3 ± 0.1

[a] calculated from released CO and CO_2,
[b] calculated from released NH_3.

The results from TPD measurements (Figure 1) confirm that the concentration of remaining carboxylic groups (CO_2-releasing groups) is the lowest for DeCACF, together with a very low concentration of CO-releasing groups, e.g. pyrone- and chromene-type structures which have a basic character. TPD profiles of $CACFNH_2$ show a peak related to NH_3-releasing groups in the temperature range of 425 K to 830 K. For CACF and DeCACF, however, this peak was not detected. Accordingly, the nitrogen content of $CACFNH_2$ was calculated as 1.1 wt%. XPS results also show that $CACFNH_2$ contains a higher nitrogen content (2.6 wt%) than CACF and DeCACF (< 0.5 wt%) and verify ethylenediamine binding to the surface as discussed in Supporting Information.

In addition, XPS results confirm that the defunctionalisation affected most strongly the carboxylic groups of CACF, however, the content of phenolic and ether units was also reduced

(see Figure 2S and related discussion in Supporting Information). Overall, DeCACF has the lowest ratio of carbon attached to oxygen per total carbon, i.e. 0.63 vs. 1.1 (CACF) and 0.93 ($CACFNH_2$) (see Table 1S).

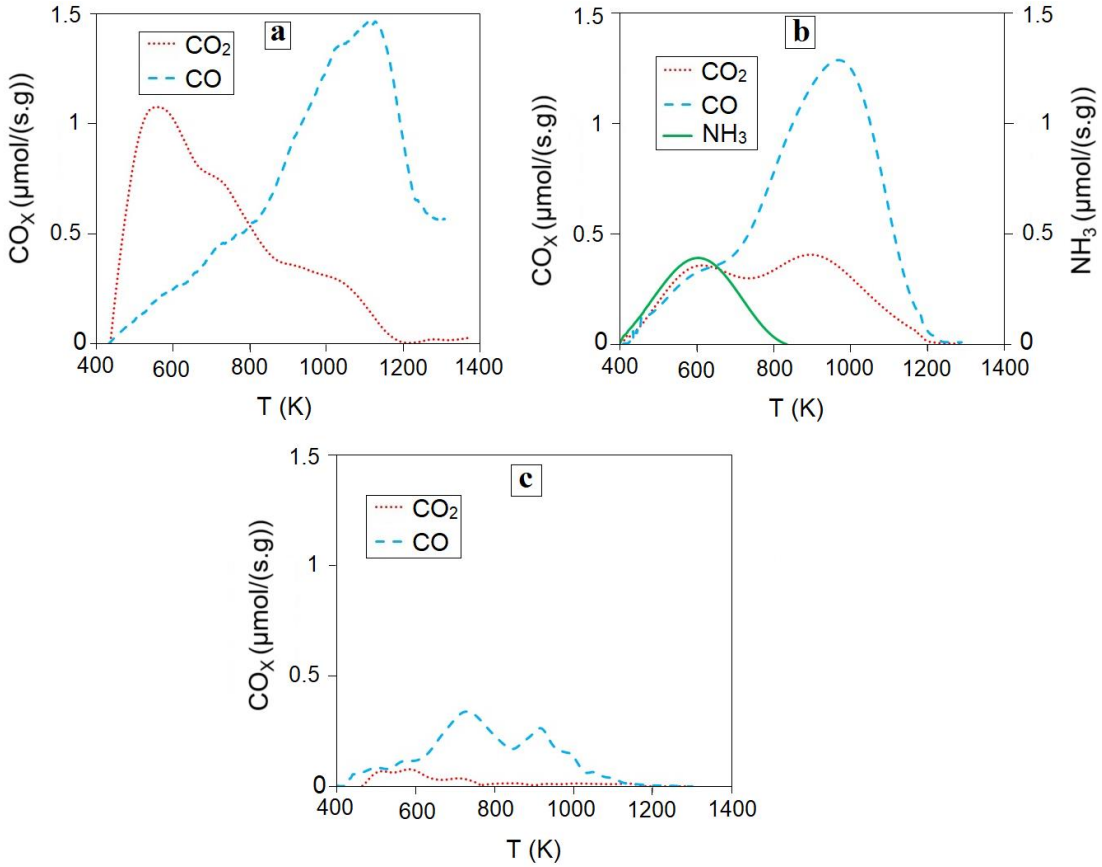

Figure 1. TPD profiles of the activated carbon felts CACF (a), $CACFNH_2$ (b) and DeCACF (c); heating rate 10 K/min.

The charge-compensating capacity of the carbon surface in adsorption of organic anions or cations can be derived from AEC and CEC, which are shown in Table 3. Amino-functionalisation slightly lowered CEC, whereas thermal defunctionalisation nearly eliminated it. At the same time, these modifications increased AEC by a factor of 2 and 4, respectively. A good correlation exists between the content of carboxylic groups (Boehm titration) and CEC which was determined at pH 7 (Figure 3S). It reveals that carboxylic groups are most relevant for CEC of the ACFs at neutral pH.

We refer the readers to Supporting Information for a more detailed discussion on surface chemical characteristics of the ACFs.

Table 3. Charge-compensation capacity of the ACFs.

Sample	Anion exchange capacity ($\mu mol/m^2$)	Cation exchange capacity ($\mu mol/m^2$)
CACF	0.054	0.79
$CACFNH_2$	0.13	0.51
DeCACF	0.20	0.021

3.2. Adsorption Experiments

3.2.1. Adsorption of PFOA, PFOS and PFBA

Adsorption isotherms of PFOA, PFOS and PFBA on the ACFs at pH 7 were determined and are shown in Figure 4S together with Freundlich and Langmuir plots in Figure 2. Table 4 lists the corresponding isotherm parameters normalised to specific surface areas of the adsorbents. The isotherm parameters were also calculated in terms of mass units and listed in Table 2S. Obviously, the adsorbents expose vastly different capacities for uptake of PFOA (Figure 2a and b). Maximum monolayer adsorption capacities (q_m) of PFOA increase significantly from 0.0044 $\mu mol/m^2$ (2.1 mg/g) on CACF to 0.18 $\mu mol/m^2$ (80 mg/g) on DeCACF. Such a substantial enhancement in adsorption capacity as observed here for the defunctionalised carbon (factor of 40) has been rarely reported before. The adsorption affinities expressed by K_F and K_L also confirm a strong improvement in adsorption of PFOA on DeCACF. Furthermore, as can be seen in Table 4, the order of the maximum loadings (q_m) and affinities (K_F and K_L) for PFOS and PFBA is the same as for PFOA: DeCACF >> $CACFNH_2$ > CACF. All these results indicate that the defunctionalisation procedure yields an adsorbent with exceptionally high affinity for uptake of both long-chain and short-chain PFAAs. This high adsorption affinity was maintained by DeCACF for at least 5 adsorption/desorption cycles of PFOA and PFBA with intermittent regeneration by methanol

extraction (see the Supporting information and Figure 5S for more details). In comparison, amidation of CACF showed only a minor improvement in adsorption of the PFAAs.

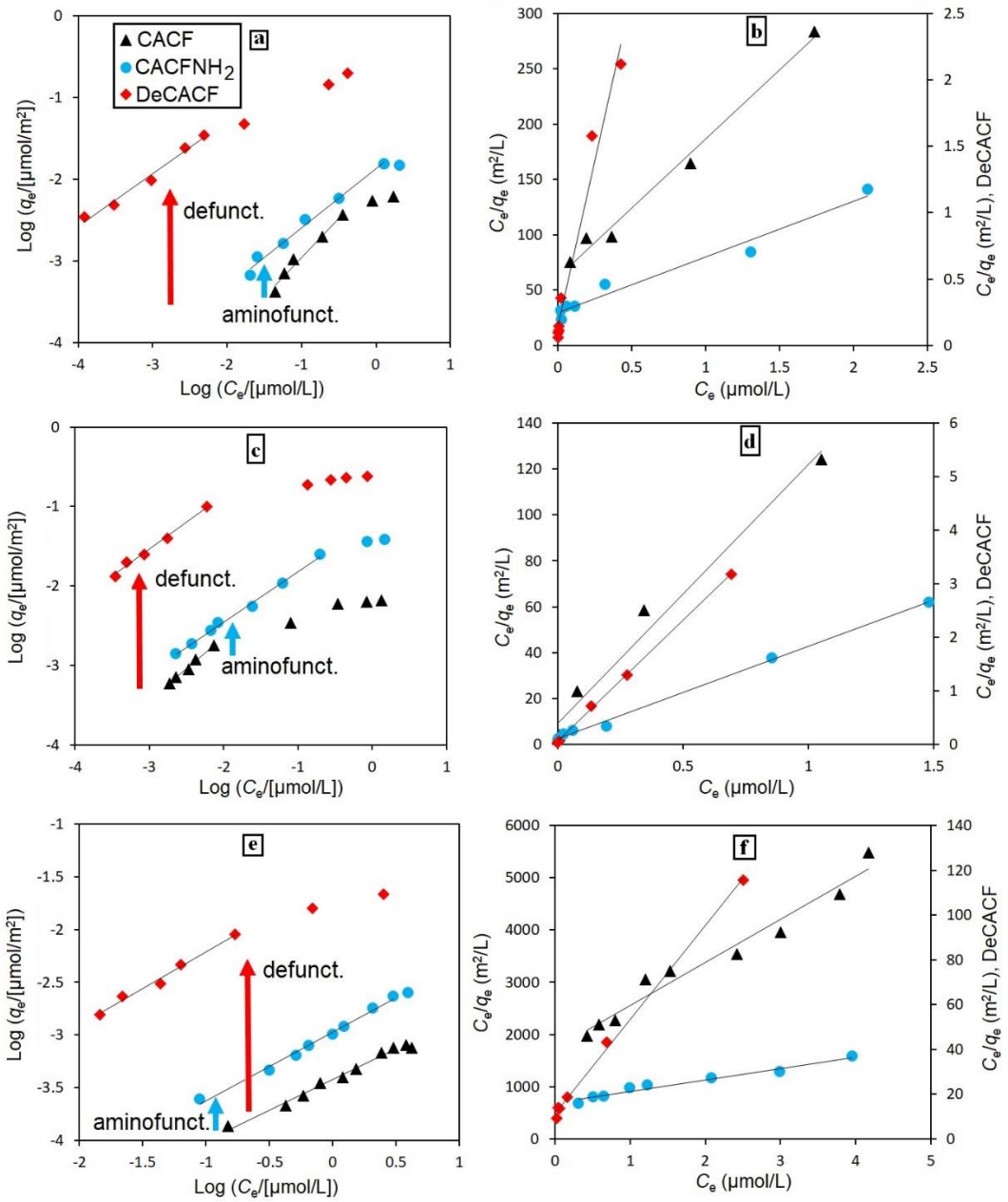

Figure 2. Experimental data on adsorption of various PFAAs on the ACFs in 10 mM Na_2SO_4 at pH 7: Freundlich and Langmuir plots (left and right, respectively) for PFOA (a and b); PFOS (c and d) and PFBA (e and f).

As mentioned earlier, amino-functionalisation and thermal defunctionalisation changed to some extent also the physical properties, i.e. specific surface area and PSD of CACF. Note that

adsorption performance was already compared by normalizing PFAA equilibrium loadings to carbon surface area (Figure 2). Figure 6S shows a plot of maximum loadings of the PFAAs versus V_p in the pore size ranges of 1-2 nm width (Figure 6Sa) and < 1 nm (Figure 6Sb). The order of maximum loadings is in agreement with neither order of available V_p in 1-2 nm width nor V_p in < 1 nm width. It seems that available V_p in a certain size fraction doesn't control the different adsorption properties of the various ACFs. An estimation of the degree of pore filling reached at the highest maximum loading gained, i.e. for PFOS on DeCACF as the best adsorbent, underlines that. According to a molar volume of PFOS (around 270 mL/mol), the maximum volumetric loading of 0.054 mL PFOS/g leads to a filling degree of 1-2 nm pores (0.16 mL/g) of only 33% at maximum (as the < 1 nm pores can also contribute to PFOS uptake). This finding clarifies that the *volume* of this micropore fraction will unlikely be the limiting factor in PFAAs adsorption. Thus, it can be concluded that the availability of pores in a certain size range cannot justify the strong difference in adsorption behaviors of the ACFs and surface chemistry is the determining factor.

Table 4. Parameters of Freundlich and Langmuir.isotherms for adsorption of PFAAs on the activate carbon felts at pH 7. [a]

		Freundlich			Langmuir		
ACF adsorbent	Adsorbate	K_F (μmol/m^2)/(μmol/L)^n	n	R^2	q_m (μmol/m^2)	K_L (L/μmol)	R^2
CACF	PFOA	0.010	0.98	0.969	0.0044	0.0048	0.986
CACF	PFOS	0.087	0.79	0.991	0.0088	0.012	0.979
CACF	PFBA	0.00038	0.58	0.989	0.0012	0.00048	0.963
$CACFNH_2$	PFOA	0.010	0.52	0.981	0.013	0.0053	0.994
$CACFNH_2$	PFOS	0.066	0.63	0.994	0.025	0.018	0.997
$CACFNH_2$	PFBA	0.0010	0.62	0.992	0.0032	0.00051	0.986
DeCACF	PFOA	0.98	0.64	0.982	0.18	0.035	0.981
DeCACF	PFOS	5.5	0.76	0.992	0.20	0.21	0.999
DeCACF	PFBA	0.031	0.70	0.987	0.024	0.0039	0.997

[a] the isotherm parameters in mass units are listed in Table 1S.

We observed in a previous study (Saeidi et al., 2020) considerable differences in adsorption loadings and affinities of PFOA and PFOS on 4 commercial ACFs, namely VS, FC15, FC10 and WK, which was subject to modification in the present study (note that WK in (Saeidi et al., 2020)

= CACF). Figures 3a and b show the maximum loadings of the PFAAs on CACF, $CACFNH_2$ and DeCACF versus AEC and CEC and include also data for the other three commercial ACFs from (Saeidi et al., 2020) (for ease of comparison, their characterisation data are included in the Supporting information (Tables 3S and 4S)).

It is a common feature for all investigated ACFs (including those investigated in (Saeidi et al., 2020)) that the three PFAAs are adsorbed according to PFOS > PFOA > PFBA. This ranking is in accordance with the general trend of higher adsorption tendency of PFAAs with increasing chain-length as reported e.g. for adsorption on fluorinated graphene sheets (Li et al., 2017), metal-organic frame- works (Liu et al., 2015), amino-functionalised cellulose (Ateia et al., 2018) and AC (Zhi and Liu, 2016).

K_d values were calculated from isotherms at the same aqueous phase concentration of $C_{e,\,PFOA}$ = 20 µg/L (0.048 µmol/L), $C_{e,\,PFOS}$ = 8 µg/L (0.016 µmol/L) and $C_{e,\,PFBA}$ = 30 µg/L (0.140 µmol/L) and plotted as surface-normalised K_d values against AEC and PZC of the ACFs in Figures 3c and 3d, respectively. It is obvious that defunctionalisation turned the worst among the commercial ACFs into the best adsorbent for the PFAAs. DeCACF as the sample with the highest AEC and PZC but lowest CEC and O-content shows the highest q_m and K_d values among all ACFs, with K_d = 2.9 L/m^2 (2.9 × 10^6 L/kg) for PFOA, 12 L/m^2 (1.2 × 10^7 L/kg) for PFOS and 0.074 L/m^2 (7.4 × 10^4 L/kg) for PFBA at the above listed C_e values. This means an enhancement in adsorption affinity of the PFAAs by up to 3 orders of magnitude in comparison with the ACF as received (CACF). Table 5S shows a comparison between adsorption coefficients of PFAAs on DeCACF and those on various adsorbents including AC materials extracted from very recent studies. This comparison proves that DeCACF has an outstanding performance in adsorption of both short- and long-chain PFAAs compared to various commercial and lab-synthesized adsorbent materials

(including Fe-based minerals, N-functionalised polymers, biochar and various activated carbon products).

Note that due to the non-linear isotherms observed for DeCACF with Freundlich n values < 1, adsorption performance increases with decreasing aqueous phase concentrations of the PFAAs. The K_d values at C_e = 0.3 µg/L which is within the environmentally relevant range reach values as high as 1.0×10^7 L/kg and 3.5×10^7 L/kg for PFOA and PFOS, respectively.

In contrast, the increased AEC of $CACFNH_2$ is not translated equivalently into increased q_m and K_d values for adsorption of the PFAAs, as this adsorbent falls out of the otherwise rather continuous correlation curves in Figures 3a and 3c. In general, adsorption of PFAAs on amino-functionalised adsorbents involves three combined factors, i.e. electrostatic interactions with functional groups of the adsorbent, hydrophobic interactions with the sorbent and sorbent morphology (Ateia et al., 2019). Possible reasons for the adsorption behaviour of PFAAs on $CACFNH_2$ are: I) Even though PZC is shifted to > 7, $CACFNH_2$ still keeps a significant density of negatively charged and thus repulsive sites for the PFAAs anions, as it still has the second-highest CEC at pH 7. Therefore, in adsorption of PFAAs on amino-functionalised AC the density of negatively charged sites on the adsorbent should be considered as a determining factor in adsorption performance of the adsorbent. II) Amino-functionalisation creates a positive charge (at near neutral pH) in a rather polar microenvironment, i.e. by units of surface–CO-NH-CH_2-CH_2-NH_3^+. Even though they provide charge compensation for the anionic head group of PFAAs, such sites might be a less suitable micro-environment for adsorption of the hydrophobic perfluoroalkyl chain. In this respect, carbon-centred positive charges resulting from proton adsorption to π-electron systems in DeCACF might be preferable. III) Amino-functionalisation, in addition, might hinder access of PFAAs to some of the pores, as the available pore opening space can be reduced

in the derivatisation. Such size exclusion is not taken into account by normalisation to BET surface areas determined from adsorption/desorption of small gas molecules (N_2, CO_2).

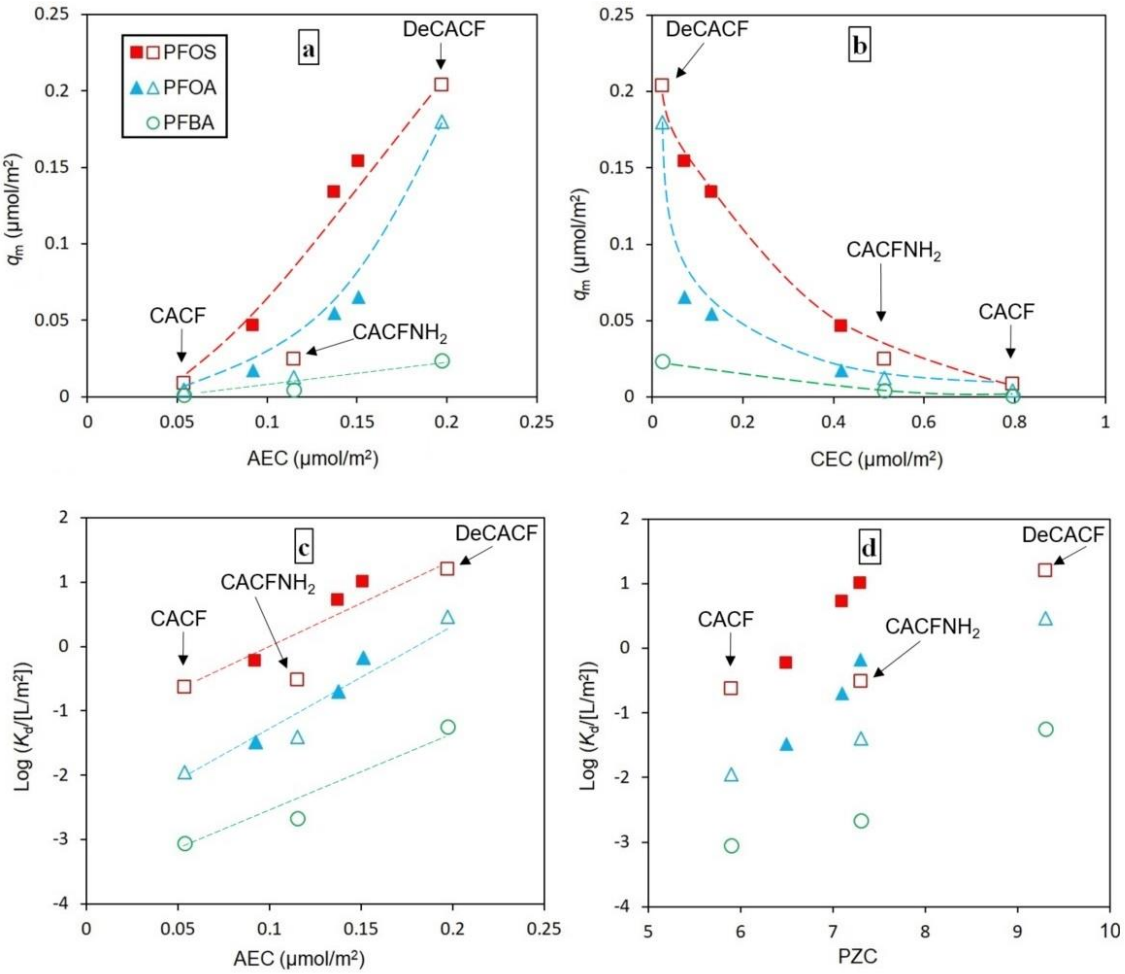

Figure 3. Correlations between maximum loadings q_m (µmol/m^2) against AEC (a), CEC (b) and between single-point adsorption coefficients log (K_d /[L/m^2]) against AEC (c) and PZC (d) for sorption of PFOA, PFOS and PFBA at pH 7. K_d values are obtained for $C_{e,\,PFOA}$ = 20 µg/L (0.05 µmol/L), $C_{e,\,PFOS}$ = 8 µg/L (0.016 µmol/L) and $C_{e,\,PFBA}$ = 30 µg/L (0.140 µmol/L). Filled symbols denote data from our previous study (Saeidi et al., 2020). Lines were added as guide to the eye.

Interestingly, $q_m \leq$ AEC holds for all ACFs and PFAAs studied. For DeCACF as best adsorbent, AEC is comparable with the maximum uptake capacity for PFOA and PFOS in terms of molar units. These results confirm the finding of our previous work indicating that the PFOA and PFOS anions can be adsorbed favourably by the interplay of hydrophobic and electrostatic

interactions when charge-balancing cationic sites are sufficiently available at the ACF surface. At the same time, the increase in q_m is much higher than the actual increase in AEC between the worst and the defunctionalised ACF as best adsorbent, which also highlights the importance of reduced repulsive interactions (decrease in CEC as shown in Figure 3b). Correlations between log K_d and PZC are shown in Figure 3d. The PZC values are 5.9 for CACF versus 7.3 for $CACFNH_2$ and 9.3 for DeCACF. PZC has been reported as a scale for the nature of electrostatic interactions between surface groups of carbon materials and PFAAs (Chen et al., 2011; Li et al., 2011; Deng et al., 2015; Chen et al., 2017): it has been stated that if pH < PZC there are electrostatic attractions between positively charged sites of the adsorbent and PFAAs, and *vice versa*. Furthermore, a review paper (Kah et al., 2017) has recently extended this evaluation to all ionisable organic compounds, including dyes (Calvete et al., 2009; Machado et al., 2011), benzoic acid (Ayranci et al., 2005) and salicylic acid (Ayranci and Duman, 2006). However, AC in general contains a wide range of functional groups having various pK_a values. For such heterogeneous surfaces, PZC cannot have the same meaning as for more homogeneous surfaces such as e.g. metal oxides or synthetic polymers with one type of functional groups (amino-functionalised polymers). In the case of a distribution of pK_a values of surface groups, a significant portion of local positive and negative charges can remain simultaneously far above and below PZC, respectively.

It can be seen from Figure 3d that even though $CACFNH_2$ has the second highest PZC among the carbon materials tested, it is still among the worst adsorbents. AEC and CEC might be more conclusive indicators of the charge density of the AC surface, as they quantify the density of charged sites at a certain relevant solution pH. Indeed, $CACFNH_2$ has the second-highest CEC at pH 7, meaning that it has still a high density of repulsive charges which are detrimental for PFAAs anion adsorption. Correlations of q_m values with CEC yield rather continuous curves which

apparently become steeper in the range of the lowest CEC values. It is obvious that a reduced density of repulsive charges should be beneficial for adsorption. However, there is also a potential cross-correlation between CEC and AEC (see Figure 7S) as C-centred basic sites are favoured (high AEC) at carbon surfaces with low density of electron-withdrawing (e.g. carboxylic) groups (low CEC).

3.2.2. Adsorption of PFOA, octanoic acid and phenanthrene

Adsorption capacities and affinities of OCA and PHE on the ACFs were determined and compared with adsorption of PFOA. Figure 8S and Tables 6S and 7S show adsorption isotherms of PHE and OCA on the ACFs and the corresponding Freundlich and Langmuir parameters. The K_d values for adsorption of the model compounds were calculated using the respective isotherm equations at C_e = 10-20 µg/L, i.e. for the low loading range where capacity limitations are negligible.

Figure 4 shows correlations between maximum loadings q_m and single point adsorption coefficients K_d in adsorption of PFOA, OCA and PHE with AEC of the ACFs. Figure 9S shows correlations of single point adsorption coefficients K_d in adsorption of the compounds with CEC, PZC and oxygen content of the ACFs. It is obvious that the three adsorbates react with different sensitivity to the changes in AC surface chemistry. PHE is rather insensitive as it shows only a slight increase in q_m for the defunctionalised carbon and nearly no change in K_d. This substantiates that changes in physical characteristics due to the modification of the carbon were of minor importance. For PHE as representative of neutral hydrophobic compounds a low surface polarity of the carbon might offer beneficial interactions; however, the overall impact of surface chemistry is low. This is also in line with experience gathered for activated carbon adsorption of "contaminants of the past", including e.g. BTEX, halogenated hydrocarbons or PAHs, where AC

performance was mainly related to porosity aspects leading to a high surface area for adsorption. In contrast, many emerging contaminants carry acidic or basic groups and are charged in the relevant pH range. PFOA and OCA (used as non-fluorinated structural analogue) are both anions at pH 7. However, they differ largely in their acid strength, with $pK_{a,\,OCA} = 4.9$ (Wellen et al., 2017) and $pK_{a,\,PFOA} = 0\text{-}1$ (Goss, 2008; Cheng et al., 2009; Baggioli et al., 2018).

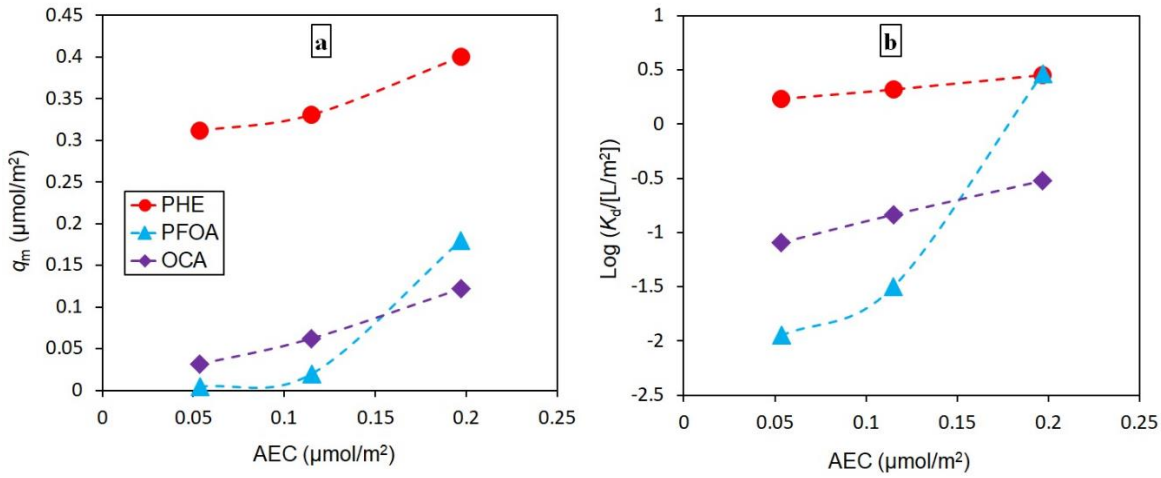

Figure 4. Correlations between maximum loadings q_m (a) and single point adsorption coefficients K_d (b) against AEC of the activated carbon felts in sorption of PFOA, OCA and PHE from 10 mM Na_2SO_4 at pH 7. K_d values are reported for $C_{e,\,PFOA}$ = 20 µg/L (0.048 µmol/L), $C_{e,\,PHE}$ = 10 µg/L (0.056 µmol/L) and $C_{e,\,OCA}$ = 10 µg/L (0.069 µmol/L). Lines were added as guide to the eye.

Both acids are much more sensitive regarding changes in surface chemistry of the ACF than PHE. In fact, PFOA reacts most strongly, i.e. with an increase in K_d by more than 2 orders of magnitude after the defunctionalisation of the ACF, whereas for OCA this enhancement is only by a factor of 4 (see Figure 4b). The maximum loading shows a similar difference: 40-fold increase for PFOA but only 3-fold increase for OCA (see Figure 4a). Thus, the question arises what is causing this stronger sensitivity of PFOA and other PFAAs towards surface chemistry of AC?

While sorptive interactions of neutral molecules include mainly non-specific van der Waals interactions, H-bonding and π-π interactions, charged molecules are also subject to attractive and

repulsive electrostatic interactions. Beyond that, removal of an ionic organic compound from the water phase into an adsorbent requires charge compensation in order to maintain phase neutrality. Likewise, adsorption of PFOA anions to the carbon surface requires either I) existence of positive charges at the surface and displacement of counter anions into the solution, or II) uptake of PFOA into the pore space together with cations to balance the pore charges. Interestingly, for all ACFs, the maximum loading for PFOA/PFOS is less than or equal to their AEC for inorganic anions. Thus, it appears that positively charged sites at the carbon surface play the major role for charge balancing at least for the tested microporous activated carbon materials.

In contrast to PFOA, OCA, due to its weaker acidity ($pK_{a,\,OCA} = 4.9$), has alternative options for obtaining charge neutrality in adsorption:

- The pK_a of OCA is closer to 7, thus a mild shift in local pH and/or pK_a close to the surface and in narrow pores (i.e. within the electric double layer) may lead to OCA protonation and finally adsorption as a neutral molecule. Nanoconfinement effects in carbon adsorbents are discussed e.g. in (Pignatello et al., 2017).
- Charge-assisted hydrogen bonding (CAHB) was suggested as an important mechanism for adsorption of organic acids/bases (Gilli and Gilli, 2000). Formation of CAHB between the carboxyl group of a solute and surface carboxyl or hydroxyl groups of the adsorbent is possible if the pK_a values of the two functional groups are comparable: surface-COO^- + H^+ + R-COO^- ↔ (surface-COO^-…H^+…$^-$OOC-R)$^-$ (Gilli and Gilli, 2000). CAHB can be understood as a charge neutralisation option, with an increase in the pK_a of the complex compared to the free acid (R-COO^-) due to a tighter constriction of the proton shared by two carboxylic groups (Pignatello et al., 2017).

By means of these mechanisms, OCA could adapt more easily than PFOA even to unfavourable negatively charged surfaces. However, if sufficient positively charged sites at a surface with an overall rather low polarity are available, as in the case of DeCACF, then OCA is outcompeted in adsorption by PFOA (and PFOS). Their sorption coefficients reach a value of PHE which is considered as well adsorbable by activated carbons. In order to understand the better adsorption of PFOA compared to OCA at DeCACF as best adsorbent, it is also interesting to compare the hydrophobicity of the two anions. Such a comparison is usually done based on octanol-water partition coefficients. However, for ionised organic compounds such as PFOA and OCA (at neutral pH), experimental values are hardly available and calculated values obtainable from the various available software tools frequently differ vastly (Kah and Brown, 2008). Note that also in case of partitioning charge neutrality of phases must be kept so that the type of counterions in the two phases and ionic strength are relevant. Thus, octanol-water partitioning coefficients are probably less applicable predictors for adsorption of ionised compounds than known from neutral compounds.

Nevertheless, based on the molecule structures one could expect a higher hydrophobicity for PFOA compared to OCA, as perfluoroalkane chains are more hydrophobic/lipophilic than alkanes as illustrated by log $K_{\mathrm{OW,\ perfluoropentane}}$ = 4.40 (C. Hansch, 1995) vs. log $K_{\mathrm{OW,\ pentane}}$ = 3.39 (Sangster, 1989). In contrast, Jing et al. suggested that the higher hydrophobicity of PFAAs is not caused by higher hydrophobicity of the fluorinated alkyl chain. Rather it results from a lower charge density at the anionic head groups (carboxylate or sulfonate) due to the strong electron withdrawing effect of the fluorinated substituent (Jing et al., 2009). Both reasons can explain the observed *partitioning* behaviour of PFAAs, but they have different consequences for interpretation

and modelling of *adsorptive* interactions. The stronger effect of the surface charge in adsorption for PFOA compared to OCA observed in this study rather speaks for a hard base head group.

To sum up, the specific importance of activated carbon surface chemistry for adsorption of PFAAs might result from their extremely low pK_a values (high acid strength) which strongly limits charge neutralization options in adsorption. In this case, positively charged surface groups in a rather non-polar environment are detrimental for providing both, charge-balancing for PFAA anionic head groups and hydrophobic interactions of the tail.

3.2.3. Effect of Competitive Ions

3.2.3.1. Inorganic Ions

Figure 5a shows K_d values for PFOA adsorption from solutions containing certain concentrations of Na_2SO_4 at circumneutral pH. Figure 10S illustrates the K_d values for adsorption of PFOS and PFBA. An increase in Na_2SO_4 concentration from 10 mM to 200 mM enhanced adsorption affinities of the PFAAs on CACF and $CACFNH_2$, whereas a slight decrease was found for DeCACF. It is known that an increase in the ionic strength of the electrolyte solution causes a compression of the electric double layer at charged surfaces, resulting in a shorter range of electrostatic repulsion or attraction forces. Thus an increase in ionic strength enhances adsorption of the PFAAs on the ACFs with CEC > AEC at pH 7 (CACF and $CACFNH_2$), where the decrease in repulsive electrostatic interactions is dominating. At the same time, a weaker and opposite trend occurs for DeCACF with CEC < AEC at pH 7, as in this case the decrease in attractive interactions is dominating. The rather small influence of high sulphate concentrations on PFOA adsorption by DeCACF speaks against a competition effect. These results confirm the view that inorganic ions cannot easily compete with strong uptake of the PFAAs exposed by the superposition of electrostatic attraction and hydrophobic interactions.

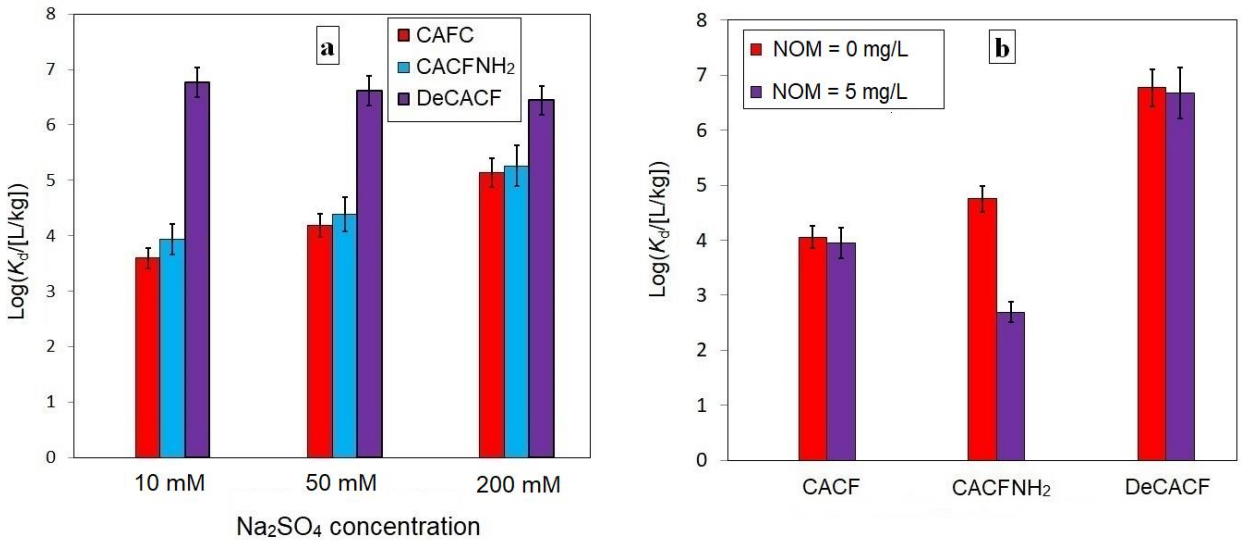

Figure 5. Effect of inorganic ions (a) and NOM (b) on sorption of PFOA. The experiments were carried out at pH 7 with C_0 = 1 mg/L PFOA. In (a) the adsorbent dosage of all ACFs were 0.1 g/L. In (b) the experiments were performed in 10 mM Na_2SO_4 with and without NOM and adsorbent dosage 0.5 g/L CACF and $CACFNH_2$ and 0.1 g/L DeCACF. The maximum deviation of single values from the mean value of 3 experiments is reported as error bars.

3.2.3.2. Natural organic matter

Surface coverage and pore blockage exposed by NOM were discussed as the main reasons that reduce adsorption of PFAAs on AC in natural water (Yu et al., 2012). In our previous study, however, we did not observe negative effects of NOM on adsorption of PFOA and PFOS on microporous ACFs at solution pH of 3 and 7. We attributed this to a size exclusion effect preventing the bulky NOM molecules from surface coverage and pore blockage (Saeidi et al., 2020). Figure 5b shows adsorption of PFOA on the ACFs at pH 7 from solution containing 5 mg/L NOM, while Figure 11S shows the results for PFOS and PFBA. In contrast to minor effects for CACF and DeCACF, $CACFNH_2$ experienced a strong reduction in PFAA adsorption in the presence of NOM. As shown in Table 1 and Figures 1Sa and 1Sb, all ACFs have comparable micropore size distributions. $CACFNH_2$ contains surface-$CONHCH_2$-CH_2-NH_3^+ units at pH 7, which obviously offer more favourable interactions with negatively charged NOM molecules (also having a moderate polarity) than the carbon-centred positive charges in DeCACF. Steric effects

could also play a role if amino-functionalisation affects pore entrances more than the inner micropore surfaces. Furthermore, considerable adsorption competition between negatively charged organic compounds and NOM has also been reported for amino-functionalised graphene oxide (Cai and Larese-Casanova, 2016). Irrespective of mechanistic interpretations, these results show that the applied defunctionalisation of the ACF improves adsorption while maintaining a high selectivity for PFAAs over NOM, even for the less hydrophobic PFBA.

3.2.4. Effect of pH value

Figure 6 shows adsorption affinities of PFOA on the ACFs at pH values 3, 7 and 9 (for all PFAAs see Figure 12S). It is obvious that adsorption affinity of DeCACF is less sensitive to changes in pH (less than a factor of 10 in K_d) than CACF and $CACFNH_2$, where K_d increased by up to 2 orders of magnitude with decreasing pH. As O-containing groups were largely removed in DeCACF, protonation/deprotonation of carboxylic (mainly within pH 3-5) and phenolic groups (mainly within pH 10-13) is of only minor importance. The Lewis base sites on DeCACF are obviously only mildly affected by an increase in pH to 9 ($pK_a \geq 9$). Therefore, adsorption affinity of the PFAAs on DeCACF is rather independent of solution pH in the range of 3 to 9. The improvement in K_d for $CACFHN_2$ compared to CACF mainly holds for pH 7, where amino-functionalisation leads to a reduced density of $–COO^-$ and the presence of $–NH_3^+$ groups. At pH 3, carboxylic groups are protonated anyway, and at pH 9, the positive charges of the amino groups are at least partly lost.

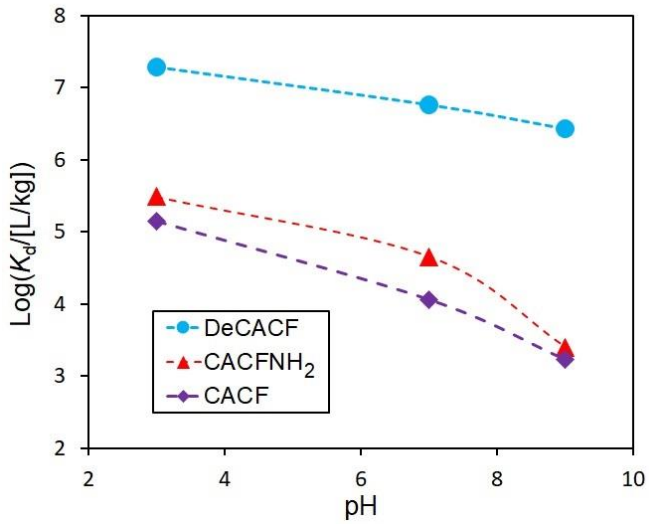

Figure 6. Effect of pH on sorption of PFOA on DeCACF, CACF and $CACFNH_2$. The experiments were carried out with C_0 = 1 mg/L of the adsorbate in 10 mM Na_2SO_4 with the following adsorbent concentrations: 0.02 g/L for DeCACF and 0.5 g/L for CACF and $CACFNH_2$. Lines were added as guide to the eye.

4. Conclusions

The comparison of adsorption affinities on various ACFs showed that the order in sensitivity to carbon surface chemistry is PFOA >> octanoic acid > phenanthrene. On the other hand, K_d and q_m for PFOA adsorption strongly correlate with the anion exchange capacity of various AC materials. Thus, charge compensation in uptake of organic ions from water into a porous adsorbents must be taken into account. Our results indicate that charge compensation provided by carbon-centered positively charged surface sites is most beneficial for PFAA anions. The extremely low pK_a of PFAAs (pK_a < 1) rules out other charge-compensation options such as a shift in protonation/deprotonation equilibria in adsorbent pores or charge-assisted hydrogen bonding which could be relevant for organic acids with typical pK_a values in the range of 4 to 5.

Defunctionalisation of a commercial ACF at 900 ˚C under hydrogen was shown to substantially enhance adsorption affinities of PFOA, PFOS and PFBA, i.e. by 3 orders of magnitude in K_d. This high adsorption affinity is rather insensitive to changes in pH as well as

competition by inorganic ions and NOM. It was maintained for at least 5 adsorption/desorption cycles of PFOA and PFBA with intermittent regeneration by methanol extraction. Activated carbon treatment by thermal defunctionalisation in presence of H_2 was shown to create a stable, basic surface nearly free of oxygen, which is obviously well suited for PFAA adsorption. It will be further optimized in future studies in terms of the balance between targeted surface modification and carbon consumption as well as the usage of forming gas (5% H_2 in N_2) for safety reasons. Defunctionalised ACF as the best adsorbent for all studied compounds exposes a superposition of electrostatic attractions and hydrophobic interactions for the organic anions. At this carbon surface, PFOA and PFOS reach the same affinity (K_d in low loading range) as phenanthrene, known as a well-adsorbing contaminant.

In contrast, amino-functionalisation by amidation of CACF increased the anion exchange capacity by only a factor of two. The improvement in PFAA adsorption was only moderate, and strongly affected by competition with NOM. Obviously, not only the presence but also the nature of basicity should be taken into account in selection of activated carbons for a highly efficient adsorption of both short- and long-chain perfluoroalkyl acids.

References

W. Shen, Z. Li, Y. Liu, Surface chemical functional groups modification of porous carbon, Recent Patents on Chemical Engineering, 1 (2008) 27–40.

Arias Espana, V.A., Mallavarapu, M., Naidu, R., 2015. Treatment technologies for aqueous perfluorooctanesulfonate (PFOS) and perfluorooctanoate (PFOA): A critical review with an emphasis on field testing. Environmental Technology & Innovation 4, 168-181.

Ateia, M., Alsbaiee, A., Karanfil, T., Dichtel, W., 2019. Efficient PFAS Removal by Amine-Functionalized Sorbents: Critical Review of the Current Literature. Environmental Science & Technology Letters 6, 688-695.

Ateia, M., Attia, M.F., Maroli, A., Tharayil, N., Alexis, F., Whitehead, D.C., Karanfil, T., 2018. Rapid Removal of Poly- and Perfluorinated Alkyl Substances by Poly(ethylenimine)-Functionalized Cellulose Microcrystals at Environmentally Relevant Conditions. Environmental Science & Technology Letters 5, 764-769.

Ayranci, E., Duman, O., 2006. Adsorption of aromatic organic acids onto high area activated carbon cloth in relation to wastewater purification. Journal of Hazardous Materials 136, 542-552.

Ayranci, E., Hoda, N., Bayram, E., 2005. Adsorption of benzoic acid onto high specific area activated carbon cloth. Journal of Colloid and Interface Science 284, 83-88.

Baggioli, A., Sansotera, M., Navarrini, W., 2018. Thermodynamics of aqueous perfluorooctanoic acid (PFOA) and 4,8-dioxa-3H-perfluorononanoic acid (DONA) from DFT calculations: Insights into degradation initiation. Chemosphere 193, 1063-1070.

Brendel, S., Fetter, É., Staude, C., Vierke, L., Biegel-Engler, A., 2018. Short-chain perfluoroalkyl acids: environmental concerns and a regulatory strategy under REACH. Environmental Sciences Europe 30, 9.
Brooke D., F.A., Nwaogu TA., 2004. Environmental Risk Evaluation Report: Perfluorooctane Sulfonate (PFOS). UK Environment Agency.
C. Hansch, A.L., and D. Hoek-man, 1995. Exploring QSAR, hydrophobic, electronic, and steric constants. Americal Chemical Society, Washington, DC.
Cai, N., Larese-Casanova, P., 2016. Application of positively-charged ethylenediamine-functionalized graphene for the sorption of anionic organic contaminants from water. Journal of Environmental Chemical Engineering 4, 2941-2951.
Calvete, T., Lima, E.C., Cardoso, N.F., Dias, S.L.P., Pavan, F.A., 2009. Application of carbon adsorbents prepared from the Brazilian pine-fruit-shell for the removal of Procion Red MX 3B from aqueous solution—Kinetic, equilibrium, and thermodynamic studies. Chemical Engineering Journal 155, 627-636.
Chen, W., Zhang, X., Mamadiev, M., Wang, Z., 2017. Sorption of perfluorooctane sulfonate and perfluorooctanoate on polyacrylonitrile fiber-derived activated carbon fibers: in comparison with activated carbon. RSC Advances 7, 927-938.
Chen, X., Xia, X., Wang, X., Qiao, J., Chen, H., 2011. A comparative study on sorption of perfluorooctane sulfonate (PFOS) by chars, ash and carbon nanotubes. Chemosphere 83, 1313-1319.
Cheng, J., Psillakis, E., Hoffmann, M.R., Colussi, A.J., 2009. Acid Dissociation versus Molecular Association of Perfluoroalkyl Oxoacids: Environmental Implications. The Journal of Physical Chemistry A 113, 8152-8156.
Deng, S., Nie, Y., Du, Z., Huang, Q., Meng, P., Wang, B., Huang, J., Yu, G., 2015. Enhanced adsorption of perfluorooctane sulfonate and perfluorooctanoate by bamboo-derived granular activated carbon. Journal of Hazardous Materials 282, 150-157.
Du, Z., Deng, S., Bei, Y., Huang, Q., Wang, B., Huang, J., Yu, G., 2014. Adsorption behavior and mechanism of perfluorinated compounds on various adsorbents—A review. Journal of Hazardous Materials 274, 443-454.
Endo, S., Goss, K.-U., 2014. Applications of Polyparameter Linear Free Energy Relationships in Environmental Chemistry. Environmental Science & Technology 48, 12477-12491.
Gagliano, E., Sgroi, M., Falciglia, P.P., Vagliasindi, F.G.A., Roccaro, P., 2020. Removal of poly- and perfluoroalkyl substances (PFAS) from water by adsorption: Role of PFAS chain length, effect of organic matter and challenges in adsorbent regeneration. Water Research 171, 115381.
Gilli, G., Gilli, P., 2000. Towards an unified hydrogen-bond theory. Journal of Molecular Structure 552, 1-15.
Goss, K.-U., 2008. The pKa Values of PFOA and Other Highly Fluorinated Carboxylic Acids. Environmental Science & Technology 42, 456-458.
Hassan, M., Liu, Y., Naidu, R., Du, J., Qi, F., 2020. Adsorption of Perfluorooctane sulfonate (PFOS) onto metal oxides modified biochar. Environmental Technology & Innovation 19, 100816.
Higgins, C.P., Field, J.A., 2017. Our Stainfree Future? A Virtual Issue on Poly- and Perfluoroalkyl Substances. Environmental Science & Technology 51, 5859-5860.
Inyang, M., Dickenson, E.R.V., 2017. The use of carbon adsorbents for the removal of perfluoroalkyl acids from potable reuse systems. Chemosphere 184, 168-175.
Ji, W., Xiao, L., Ling, Y., Ching, C., Matsumoto, M., Bisbey, R.P., Helbling, D.E., Dichtel, W.R., 2018. Removal of GenX and Perfluorinated Alkyl Substances from Water by Amine-Functionalized Covalent Organic Frameworks. Journal of the American Chemical Society 140, 12677-12681.
Jing, P., Rodgers, P.J., Amemiya, S., 2009. High Lipophilicity of Perfluoroalkyl Carboxylate and Sulfonate: Implications for Their Membrane Permeability. Journal of the American Chemical Society 131, 2290-2296.
Kah, M., Brown, C.D., 2008. LogD: Lipophilicity for ionisable compounds. Chemosphere 72, 1401-1408.
Kah, M., Sigmund, G., Xiao, F., Hofmann, T., 2017. Sorption of ionizable and ionic organic compounds to biochar, activated carbon and other carbonaceous materials. Water Research 124, 673-692.
Karickhoff, S.W., 1981. Semi-empirical estimation of sorption of hydrophobic pollutants on natural sediments and soils. Chemosphere 10, 833-846.
Li, F., Wei, W., Gao, D., Xia, Z., 2017. The adsorption behavior and mechanism of perfluorochemicals on oxidized fluorinated graphene sheets supported on silica. Analytical Methods 9, 6645-6652.
Li, X., Chen, S., Quan, X., Zhang, Y., 2011. Enhanced Adsorption of PFOA and PFOS on Multiwalled Carbon Nanotubes under Electrochemical Assistance. Environmental Science & Technology 45, 8498-8505.
Liu, K., Zhang, S., Hu, X., Zhang, K., Roy, A., Yu, G., 2015. Understanding the Adsorption of PFOA on MIL-101(Cr)-Based Anionic-Exchange Metal–Organic Frameworks: Comparing DFT Calculations with Aqueous Sorption Experiments. Environmental Science & Technology 49, 8657-8665.

Long, L., Hu, X., Yan, J., Zeng, Y., Zhang, J., Xue, Y., 2019. Novel chitosan–ethylene glycol hydrogel for the removal of aqueous perfluorooctanoic acid. Journal of Environmental Sciences 84, 21-28.
Machado, F.M., Bergmann, C.P., Fernandes, T.H.M., Lima, E.C., Royer, B., Calvete, T., Fagan, S.B., 2011. Adsorption of Reactive Red M-2BE dye from water solutions by multi-walled carbon nanotubes and activated carbon. Journal of Hazardous Materials 192, 1122-1131.
McCleaf, P., Englund, S., Östlund, A., Lindegren, K., Wiberg, K., Ahrens, L., 2017. Removal efficiency of multiple poly- and perfluoroalkyl substances (PFASs) in drinking water using granular activated carbon (GAC) and anion exchange (AE) column tests. Water Research 120, 77-87.
Menéndez, J.A., Phillips, J., Xia, B., Radovic, L.R., 1996. On the Modification and Characterization of Chemical Surface Properties of Activated Carbon: In the Search of Carbons with Stable Basic Properties. Langmuir 12, 4404-4410.
Phong Vo, H.N., Ngo, H.H., Guo, W., Hong Nguyen, T.M., Li, J., Liang, H., Deng, L., Chen, Z., Hang Nguyen, T.A., 2020. Poly-and perfluoroalkyl substances in water and wastewater: A comprehensive review from sources to remediation. Journal of Water Process Engineering 36, 101393.
Pignatello, J.J., Mitch, W.A., Xu, W., 2017. Activity and Reactivity of Pyrogenic Carbonaceous Matter toward Organic Compounds. Environmental Science & Technology 51, 8893-8908.
Qiu, L., Chen, Y., Yang, Y., Xu, L., Liu, X., 2013. A Study of Surface Modifications of Carbon Nanotubes on the Properties of Polyamide 66/Multiwalled Carbon Nanotube Composites. Journal of Nanomaterials 2013, 8.
Rahman, M.F., Peldszus, S., Anderson, W.B., 2014. Behaviour and fate of perfluoroalkyl and polyfluoroalkyl substances (PFASs) in drinking water treatment: A review. Water Research 50, 318-340.
Saeidi, N., Kopinke, F.-D., Georgi, A., 2020. Understanding the effect of carbon surface chemistry on adsorption of perfluorinated alkyl substances. Chemical Engineering Journal 381, 122689.
Sangster, J., 1989. Octanol-Water Partition Coefficients of Simple Organic Compounds. Journal of Physical and Chemical Reference Data 18, 1111-1229.
Shafeeyan, M.S., Daud, W.M.A.W., Houshmand, A., Shamiri, A., 2010. A review on surface modification of activated carbon for carbon dioxide adsorption. Journal of Analytical and Applied Pyrolysis 89, 143-151.
Sigmund, G., Gharasoo, M., Hüffer, T., Hofmann, T., 2020. Deep Learning Neural Network Approach for Predicting the Sorption of Ionizable and Polar Organic Pollutants to a Wide Range of Carbonaceous Materials. Environmental Science & Technology 54, 4583-4591.
Sörengård, M., Östblom, E., Köhler, S., Ahrens, L., 2020. Adsorption behavior of per- and polyfluoralkyl substances (PFASs) to 44 inorganic and organic sorbents and use of dyes as proxies for PFAS sorption. Journal of Environmental Chemical Engineering 8, 103744.
Sznajder-Katarzyńska, K., Surma, M., Cieślik, I., 2019. A Review of Perfluoroalkyl Acids (PFAAs) in terms of Sources, Applications, Human Exposure, Dietary Intake, Toxicity, Legal Regulation, and Methods of Determination. Journal of Chemistry 2019, 2717528.
T. Pancras, G.S., T. Held, K. Baker, I. Ross, H. Slenders, M.J. Spence, 2016. Environmental fate and effects of polyand perfluoroalkyl substances (PFAS). ARCADIS, Brussels.
Teaf, C.M., Garber, M.M., Covert, D.J., Tuovila, B.J., 2019. Perfluorooctanoic Acid (PFOA): Environmental Sources, Chemistry, Toxicology, and Potential Risks. Soil and Sediment Contamination: An International Journal 28, 258-273.
Walters, R.W., Luthy, R.G., 1984. Equilibrium adsorption of polycyclic aromatic hydrocarbons from water onto activated carbon. Environmental Science & Technology 18, 395-403.
Wellen, B.A., Lach, E.A., Allen, H.C., 2017. Surface pKa of octanoic, nonanoic, and decanoic fatty acids at the air–water interface: applications to atmospheric aerosol chemistry. Physical Chemistry Chemical Physics 19, 26551-26558.
Yu, J., Lv, L., Lan, P., Zhang, S., Pan, B., Zhang, W., 2012. Effect of effluent organic matter on the adsorption of perfluorinated compounds onto activated carbon. Journal of Hazardous Materials 225-226, 99-106.
Zhang, J., Zhang, Y., Yu, S., Tang, Y., 2016. Sorption characteristics of tetrabromobisphenol A by oxidized and ethylendiamine-functionalized multi-walled carbon nanotubes. Desalination and Water Treatment 57, 17343-17354.
Zhi, Y., Liu, J., 2015. Adsorption of perfluoroalkyl acids by carbonaceous adsorbents: Effect of carbon surface chemistry. Environmental Pollution 202, 168-176.
Zhi, Y., Liu, J., 2016. Surface modification of activated carbon for enhanced adsorption of perfluoroalkyl acids from aqueous solutions. Chemosphere 144, 1224-1232.

Supporting information

What is specific in adsorption of perfluoroalkyl acids on carbon materials?

Navid Saeidi, Frank-Dieter Kopinke, Anett Georgi *

Helmholtz Centre for Environmental Research – UFZ, Department of Environmental Engineering, D-04318 Leipzig, Germany

Corresponding author contact information: Tel.: +49 341 235 1760; Fax: +49 341 235 1471; E-mail: anett.georgi@ufz.de

(19 Pages, 7 Tables and 12 Figures)

Discussion on physical properties of the ACFs:

Figure 1Sa shows a comparison between pore size distributions (PSD) of the ACFs and that of a coal-derived commercial powder AC (Chemviron). The results show that the pores of CACF, $CACFNH_2$ and DeCACF are predominantly in the micropore range, whereas Chemviron AC exposes a broader distribution, including micro-, meso- and macropores. **Figure 1Sb** illustrates the PSD of the activated carbon felts obtained by CO_2 sorption at 0 °C.

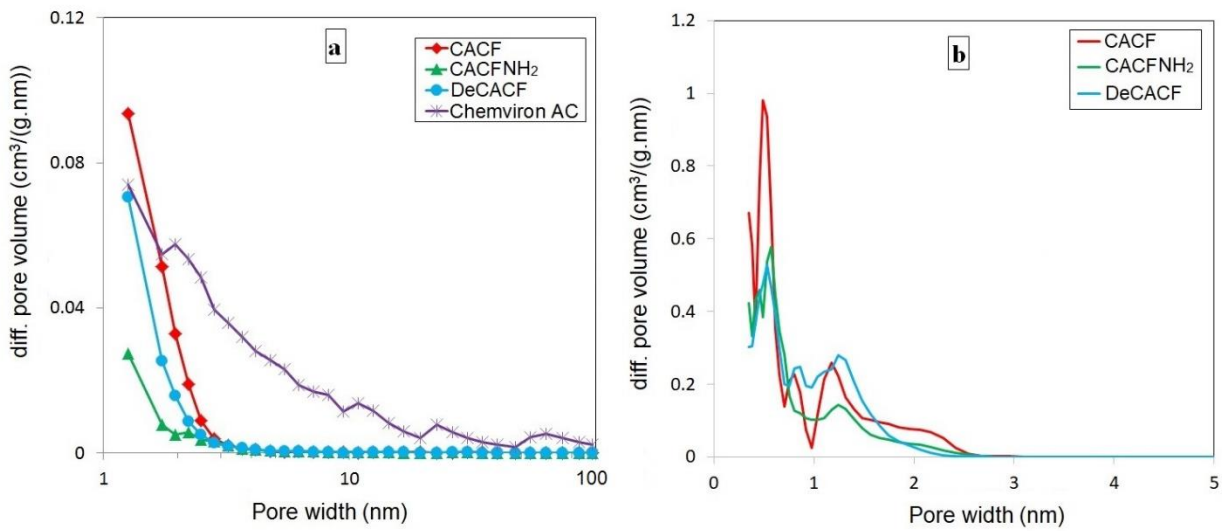

Figure 1S. Pore size distributions of the ACFs and Chemviron powder AC: a) analysis of mesopores obtained from N_2 sorption data and BJH model; b) analysis of micropores obtained from CO_2 sorption data and NLDFT analysis.

In general, amino-functionalisation reduced the total pore volume by 40% whereas defunctionalisation of the ACF led to only 15% loss (see Table 1). The decrease in the fibre diameter from 12 to 6.5 µm reveals that the thermal defunctionalisation is inherently accompanied by a significant loss of AC material. The ACFs are mostly microporous in contrast to a commercial powder AC which has a wider PSD (Figure 1Sa). Figure 1Sb shows the PSD of the ACFs in the micropore range. All ACFs have a comparable bimodal PSD in the micropore range. However, the respective proportions of V_p are different. CACF has a 60/40 distribution of V_p in the two size ranges, < 1 nm and 1-2 nm. Defunctionalisation mainly widened the most narrow pores < 1 nm, whereas amino-functionalisation reduced the V_p in both size ranges, thus leading to about 30% decrease in specific surface area.

The missing share of larger pores in ACFs could be considered as a potential disadvantage with respect to a slower sorption kinetics. However, it is partly compensated for by the small fibre thickness, which means that the diffusion distances can be kept short.

Discussion on chemical surface properties of the ACFs:

As it can be seen in Table 2, amino-functionalisation didn't affect significantly the content of weakly acidic groups (phenols, lactones and lactols). Due to the high pK_a (10 to 13 (Bandosz et al., 1993)), phenols do not play a role for surface net charge at near-neutral pH. On the other hand, protonation/deprotonation equilibria of lactones and lactols (pK_a in the range of 6 to 10 (Gómez-Bombarelli et al., 2013)) can be relevant for surface net charge under the conditions applied in our experiments (pH 3 to 7).

Figure 2S shows C 1s XPS spectra of the various ACFs as well as the N 1s spectrum for $ACFNH_2$. For CACF and DeCACF, five forms of carbon occurring on the surface were considered in the deconvolution of the C 1s XPS spectra (**Figure 2Sa** and **b**), although one additional type originating from C−N structures was recorded solely for $CACFNH_2$ (**Figure 2Sc**). Bands characteristic for carbon occurring in graphite (284.2-284.9 eV (Polovina et al., 1997)), phenols, ethers or alcohols (285.4-286.3 eV (Polovina et al., 1997)), carbonyls or quinones (287.2-287.9 eV (Polovina et al., 1997)), bonded to nitrogen structures (286.3-287.5 eV (Polovina et al., 1997)), carboxylic groups or esters (288.7-289.3 eV (Polovina et al., 1997)) are detected (see **Table 1S**). Furthermore, the band in the range 290.2 to 290.8 eV was contributed to carbonates, occluded CO or π-electrons in aromatic rings (Hontoria-Lucas et al., 1995).

The band of surface-bound ethylenediamine in XPS spectra can be deconvoluted with three peaks as observed for ethylenediamine-functionalised carbon nanotubes (Keen et al., 2006) and graphene oxide (Cai and Larese-Casanova, 2016); this also applies to $CACFNH_2$ (**Figure 2Sd**). In particular, the terminal $C{-}NH_2$ group (peak at 399.3 eV), and the amide group HN−C=O (peak at 400 eV) formed with the carbon surface can be observed. From the ethylenediamine structure it was expectable that the ratio of these peak areas is around 1:1 (Keen et al., 2006; Cai and Larese-Casanova, 2016). The amide formation reduces the carboxylic surface group concentration on $CACFNH_2$ compared to CACF (see results from Boehm titration and C 1s XPS). A third smaller peak in the N 1s spectrum occurs (at 401.7 eV). Keen et al. (Keen et al., 2006) reported that this peak is caused by ion pair formation between protonated ethylenediamine and carboxylate groups.

Obviously, some noncovalently bound ethylenediamine stays within the adsorbent even after exhaustive washing.

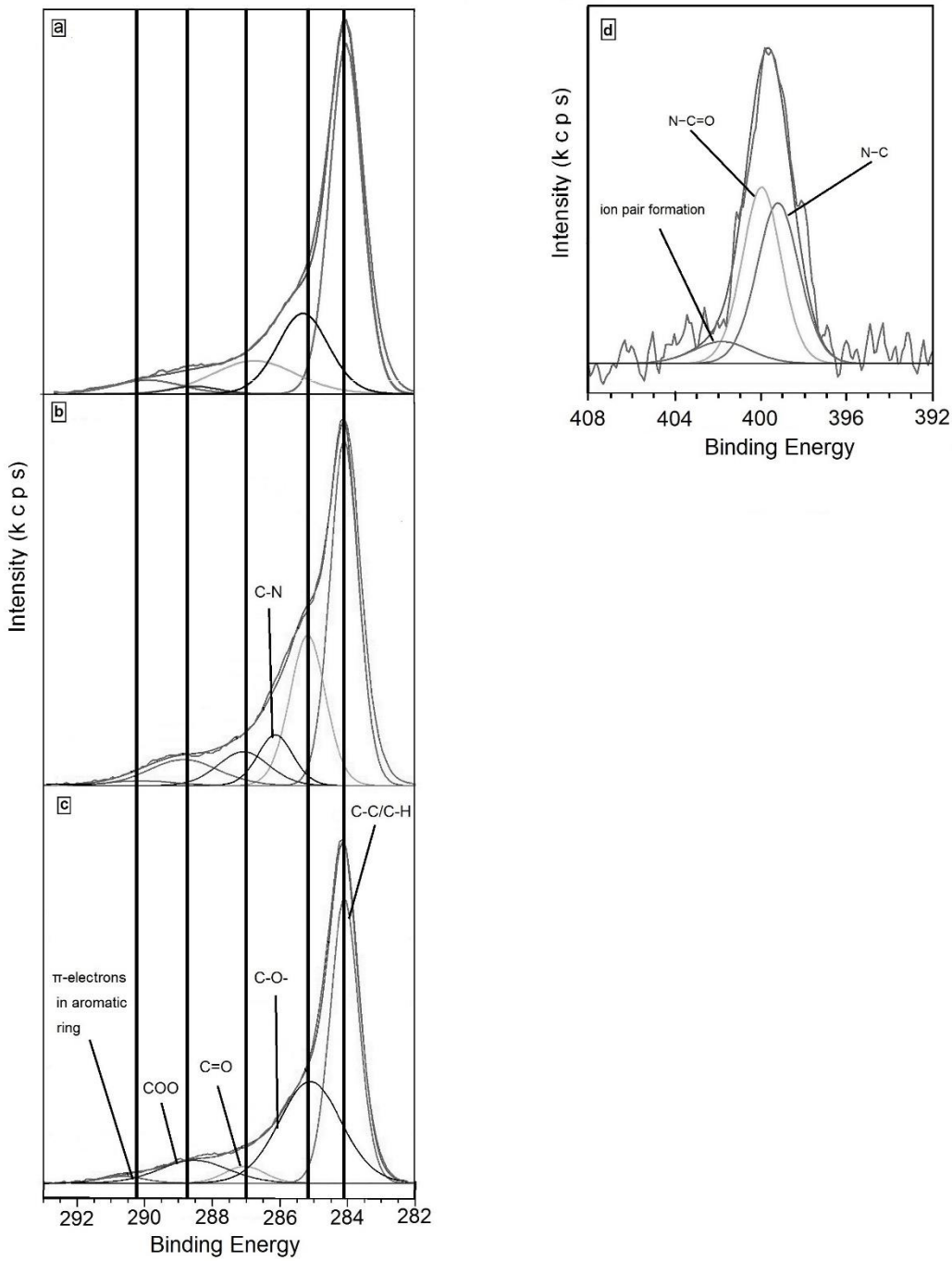

Figure 2S. Deconvoluted C 1S XPS spectra of CACF (a), $CACFNH_2$ (b) and DeCACF (c) as well as N 1S XPS spectrum of $CACFNH_2$ (d). Results are given in Table 1S.

Table 1S. Fraction of functional groups in C 1s and N 1s XPS spectra of activated carbon felts.

Sample	C^a_{ox}/C_{total}	C 1s peak (relative area %)						N 1s peak (relative area %)		
		C in graphite	Phenol / ether	C−N	Carbonyl / quinone	Carboxyl	Others	Amine	Amide	Ion pair formation
CACF	1.1	48.0	37.0	-	4.0	9.0	2.0	-	-	-
$CACFNH_2$	0.93	47.0	34.6	6.2	4.1	6.1	2.0	45.5	46.0	8.5
DeCACF	0.63	61.2	20.8	-	9.0	1.9	6.9	-	-	-

[a] carbon attached to oxygen.

The original CACF has a PZC as low as 5.9, thus at pH 7 its net surface charge is negative. Amino-functionalisation shifted the PZC to 7.3 whereas defunctionalisation caused a stronger shift to 9.3. A very low concentration of acidic groups coupled with a high concentration of C-centred basic sites provide DeCACF with this high PZC. The amidation procedure binds ethylenediamine to carboxylic groups; however, it is obviously incomplete as around 55% of carboxylic groups are remaining (based on Boehm titration results). Thus, the basic sites created (free amine group of ethylenediamine with $pK_{a1} = 9.9$) just balance the remaining carboxylic groups, resulting in a PZC close to 7.

The high PZC and thus basic character of DeCACF combined with its low O content, as confirmed by the characterisation methods described above, highlights the role of basicity related to the carbon backbone itself, i.e. π-electron-rich sites. In fact, we supported the presence of these sites on DeCACF by removing acidic groups and saturating any resulting reactive radical sites with hydrogen.

Figure 3S compares CEC and carboxylic groups' concentrations (determined by Boehm titration) of the ACFs.

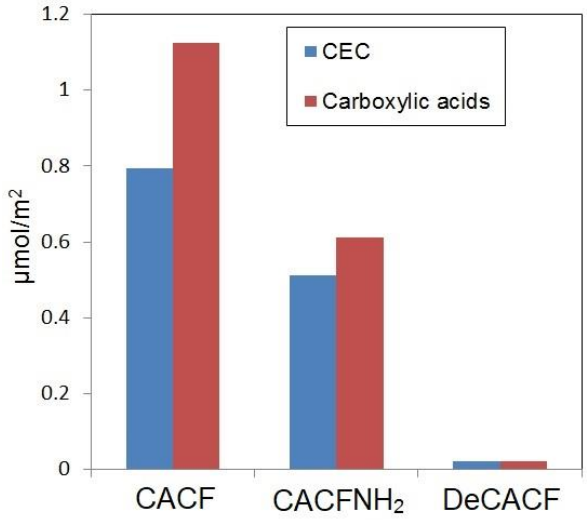

Figure 3S. Comparison between CEC and concentrations of carboxylic groups of the ACFs.

Adsorption of PFOA, PFOS and PFBA:

Figure 4S shows experimental adsorption isotherms of PFOA, PFOS and PFBA on the ACFs at pH 7.

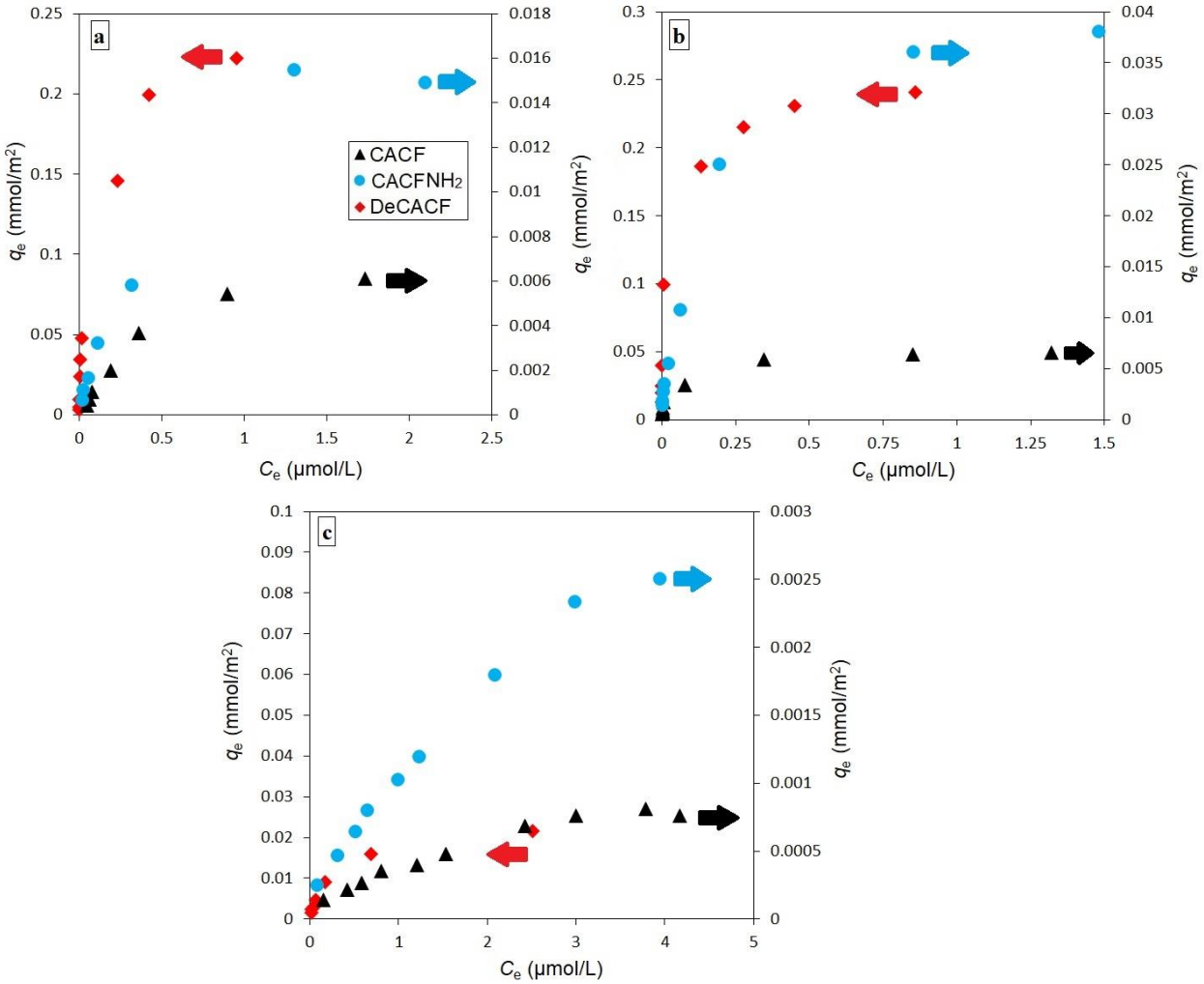

Figure 4S. Experimental data on adsorption of PFOA (a), PFOS (b) and PFBA (c) on the ACFs in 10 mM Na_2SO_4 at pH 7.

Table 2S shows the isotherm parameters collected in Table 5 of the main part in terms of mass units.

Table 2S. Isotherm parameters of Freundlich and Langmuir for sorption of PFOA, PFOS and PFBA in terms of mass units.

		Freundlich			Langmuir		
ACF adsorbent	Adsorbate	K_F (mg/g)/(mg/L)^n	n	R^2	q_m (mg/g)	K_L (L/g)	R^2
CACF	PFOA	1.00	0.98	0.977	2.1	11,500	0.986
CACF	PFOS	83	0.79	0.991	5.0	25,000	0.979
CACF	PFBA	0.22	0.58	0.989	0.29	2,200	0.963
$CACFNH_2$	PFOA	4.90	0.52	0.981	3.70	12,300	0.994
$CACFNH_2$	PFOS	37	0.63	0.994	8.9	36,000	0.997
$CACFNH_2$	PFBA	0.41	0.62	0.992	0.49	2,400	0.989
DeCACF	PFOA	710	0.64	0.983	80	79,000	0.981
DeCACF	PFOS	4,700	0.76	0.992	103	420,000	0.999
DeCACF	PFBA	19	0.70	0.987	5.1	17,200	0.997

Figure 5S shows adsorption of PFOA and PFBA on DeCACF in 5 successive adsorption-regeneration cycles. In brief, after the first adsorption step, the adsorbent (DeCACF) was immersed in pure methanol (1 g DeCACF in 1 L methanol) and shaken for 2 days. Then, the adsorbent was separated from methanol and dried. After that, the second adsorption cycle was performed by preparing the same adsorption condition as the first step, e.g. 0.1 g/L of adsorbent dosage for PFOA and 0.5 g/L for PFBA in 10 mM Na_2SO_4 at pH around 7 plus 1 mg/L of adsorbates for 2 days. It is worth pointing out that desorption percentage, which was calculated by C_e of PFOA (or PFBA) after adsorption and C_e of PFOA (or PFBA) after desorption at the same cycle, was for all cycles > 90%, i.e. adsorption was largely reversible.

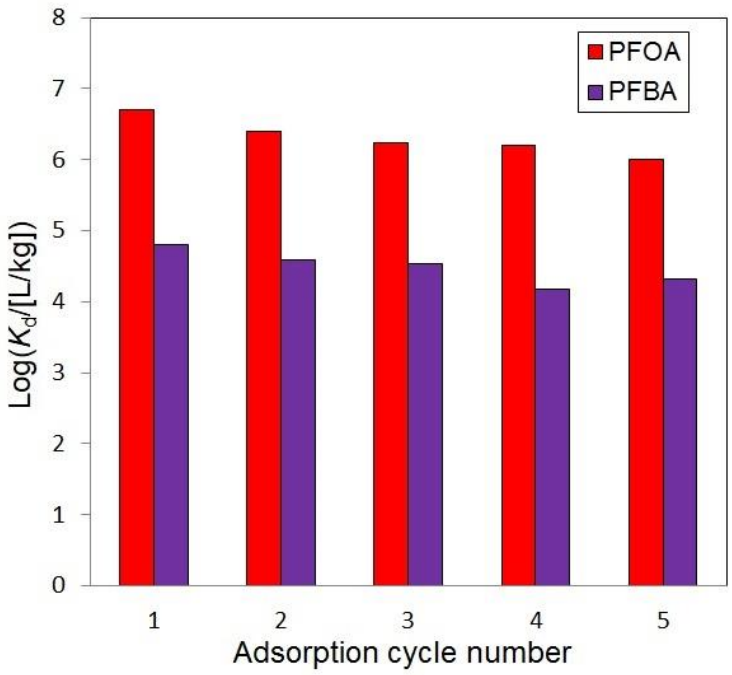

Figure 5S. Adsorption of PFOA and PFBA on DeCACF in 5 cycles. Experimental condition: adsorbent dosage: 0.1 g/L for PFOA and 0.5 g/L for PFBA; C_0 = 1 mg/L, electrolyte: 10 mM Na_2SO_4 at pH = 6.8 ± 0.4.

Figure 6S shows the effect of PSD on adsorption capacities of PFAAs on the ACFs.

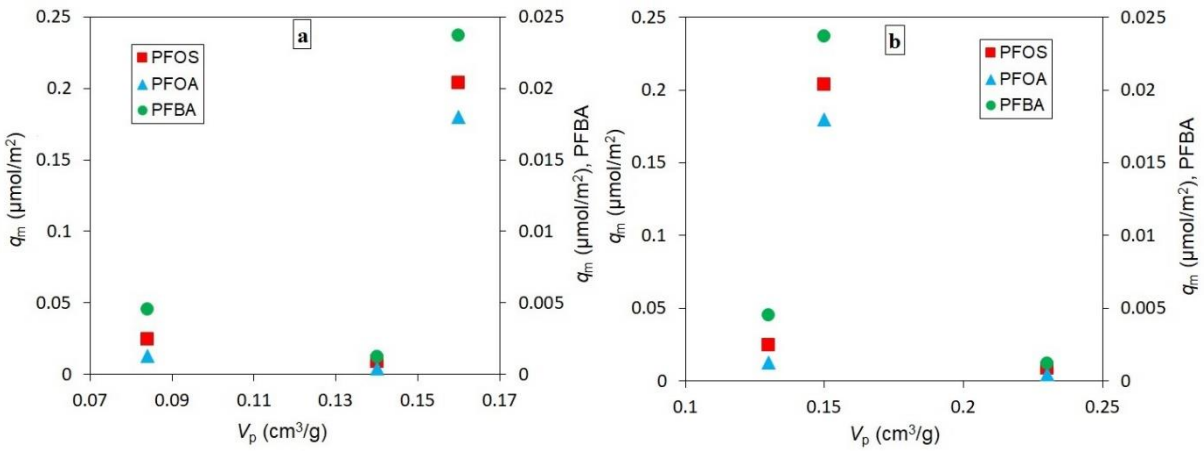

Figure 6S. Maximum loadings in adsorption of PFAAs versus volume of pores with (a) 1-2 nm width and (b) width < 1 nm.

Tables 3S and **4S** list physical properties and surface chemical properties of three commercial ACFs which were applied for sorption of PFOA and PFOS in our previous study (Saeidi et al., 2020).

Table 3S. Physical properties of the commercial ACFs from our previous study (Saeidi et al., 2020).

Sample	BET surface area (m^2/g) [a]	Total pore volume (cm^3/g) [a]	Pore volume (1-2 nm pore width) [b]	Pore volume (< 1 nm pore width) [b]	Fiber diameter (μm) [c]
VS	2100	0.99	0.57	0.23	10 ± 1
FC15	1600	0.74	0.47	0.13	10 ± 2
FC10	1400	0.62	0.34	0.21	12 ± 1

[a] obtained from nitrogen adsorption/desorption, [b] obtained from CO_2 sorption,
[c] an average of 10 measurements was reported.

Table 4S. Surface chemical properties of the commercial ACFs from our previous study (Saeidi et al., 2020).

Sample	Boehm Titration				TPD			N-content[b]	PZC	AEC	CEC
	pK_a ~ 3-6	pK_a ~ 6-10	pK_a ~ 10-13	pK_a ~ 3-13							
	Carboxylic acids	Lactons and lactols	Phenols	Total acidity	CO	CO_2	O-content[a]				
	(μmol/m^2)						(wt%)			(μmol/m^2)	
VS	0.0386	0.124	0.0667	0.229	0.338	0.192	2.5	0.2	7.3	0.148	0.0714
FC15	0.0687	0.0750	0.287	0.431	1.19	0.169	3.9	0.5	7.1	0.137	0.131
FC10	0.298	0.0992	0.695	1.09	4.22	1.13	15.9	0.6	6.5	0.0922	0.418

[a] obtained from released CO and CO_2, [b] determined by means of XPS analysis.

Table 5S compares performance of DeCACF in adsorption of PFAAs with adsorption performance of various adsorbents including AC materials from very recently published studies. This comparison is based on single-point adsorption coefficients (K_d) at a certain equilibrium aqueous phase concentration (C_e) of the PFAAs. We calculated the K_d values from isotherm plots and Freundlich isotherm parameters reported in the respective studies. Sörengård et al. didn't report adsorption isotherms but K_d values in their adsorption experiments. From K_d values and other information provided by the authors, e.g. initial concentration of the adsorbates, adsorbent dosage and solution volume, we calculated C_e for the corresponding K_d values. Data were selected in order to provide comparable C_e for the various adsorbents for each solute, i.e. PFOA, PFOS and PFBA.

Table 5S. A comparison between single-point adsorption coefficients (K_d) of PFAAs on DeCACF with those on various adsorbents reported very recently in literature.

Adsorbent	PFAAs	K_d (L/kg)	C_e (µg/L)	pH	Reference
DeCACF	PFOA	2.9×10^6	20	7	This work
poly(ethylenimine)-functionalised cellulose	PFOA	6.3×10^5	20	6.5	(Ateia et al., 2018)
GAC [a]	PFOA	1.3×10^5	30	7	(Zhang et al., 2019)
Biochar [b]	PFOA	8.2×10^4	40	7	(Zhang et al., 2019)
Powder AC [c, *]	PFOA	5.6×10^3	6.7	7.5	(Sörengård et al., 2020)
GAC [d, *]	PFOA	3.1×10^4	1.3	7.5	(Sörengård et al., 2020)
Nanoscale zerovalent iron	PFOA	1.8×10^3	20	8.3	(Zhang et al., 2018)
DeCACF	PFOS	1.2×10^7	8	7	This work
GAC [a]	PFOS	5.1×10^5	10	7	(Zhang et al., 2019)
Biochar [b]	PFOS	4.3×10^5	10	7	(Zhang et al., 2019)
Powder AC [c, *]	PFOS	1.0×10^4	3.8	7.5	(Sörengård et al., 2020)
GAC [d, *]	PFOS	1.0×10^4	4	7.5	(Sörengård et al., 2020)
Nanoscale zerovalent iron (nZVI)	PFOS	8.7×10^4	2.5	8.6	(Zhang et al., 2018)
Sulfidated nZVI	PFOS	5.9×10^4	2.5	8.3	(Zhang et al., 2018)
γ-FeOOH	PFOS	8.3×10^4	2.5	7.4	(Zhang et al., 2018)
DeCACF	PFBA	7.4×10^4	30	7	This work
GAC [a]	PFBA	5.5×10^3	150	7	(Zhang et al., 2019)
Biochar [b]	PFBA	6.9×10^3	150	7	(Zhang et al., 2019)
Powder AC [c, *]	PFBA	9.1×10^1	82	7.5	(Sörengård et al., 2020)
GAC [d, *]	PFBA	1.3×10^3	23	7.5	(Sörengård et al., 2020)

[a] Fisher Scientific (USA), [b] Biochar Supreme Inc. (USA), [c] NORIT® A ULTRA E 153 (Sweden), [d] Calgon Carbon (Sweden). [*] The two best-performing adsorbent materials in terms of PFOA adsorption (named GAC 2 and PAC 2 there) were selected for comparison from a study of 44 sorbent materials (Sörengård et al., 2020). Adsorption was performed from a mix of per- and polyfluoroalkyl substances (PFAS) (n=17). The total adsorbent loadings with PFAS are < 0.04 mg/g (1.7 mg/L total PFAS and 2.5 g/L adsorbent applied = 0.68 mg/g = 0.068 wt%). Due to this extremely low loading, adsorption competition unlikely plays a determining role in these experiments.

Figure 7S shows a plot of anion exchange capacities (AEC) and cation exchange capacities (CEC) versus point of zero net proton charges (PZC).

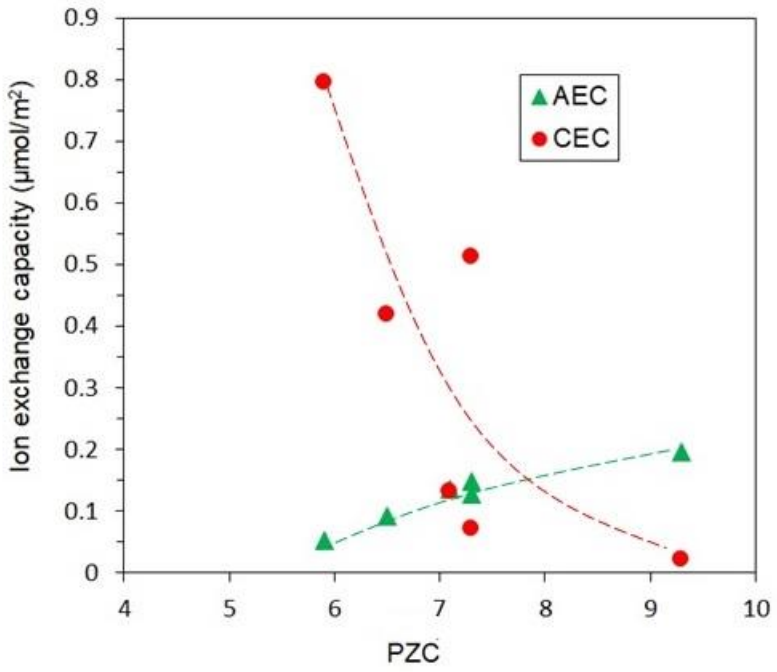

Figure 7S. AEC and CEC (µmol/m^2) versus PZC of the ACFs. Lines were added as guide to the eye.

Adsorption of PHE and OCA:

Figure 8S shows the experimental data in adsorption of PHE and OCA on CACF, $CACFNH_2$ and DeCACF fitted with Langmuir and Freundlich equations.

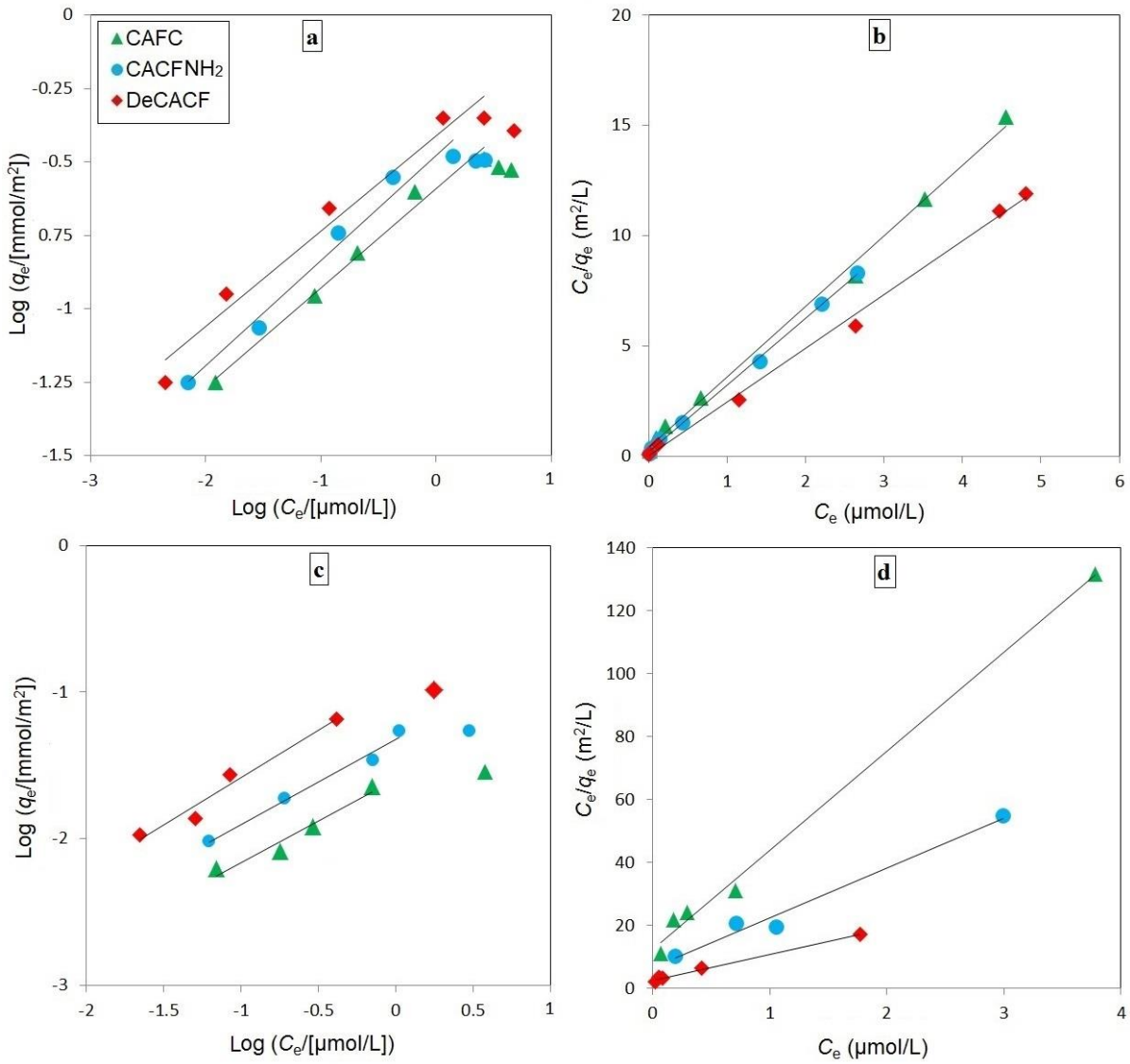

Figure 8S. Sorption isotherms for PHE on the ACFs fitted by Freundlich (a) and Langmuir (b) and for OCA fitted by Freundlich (c) and Langmuir (d) equations.

Tables 6S and **7S** list the isotherm parameters based on specific surface areas and in mass units of the ACFs, respectively.

Table 6S. Isotherm parameters in sorption of PHE and OCA normalized to specific surface areas.

		Freundlich			Langmuir		
ACF adsorbent	Adsorbate	K_F (μmol/m^2)/(μmol/L)^n	n	R^2	q_m (μmol/m^2)	K_L (L/μmol)	R^2
CACF	PHE	0.26	0.34	0.987	0.31	0.0081	0.996
$CACFNH_2$	PHE	0.33	0.35	0.978	0.33	0.014	0.998
DeCACF	PHE	0.45	0.36	0.983	0.43	0.030	0.997
CACF	OCA	0.026	0.56	0.950	0.032	0.0026	0.995
$CACFNH_2$	OCA	0.048	0.58	0.984	0.062	0.0028	0.983
DeCACF	OCA	0.12	0.64	0.965	0.12	0.0031	0.992

Table 7S. Isotherm parameters in sorption of PHE and OCA in terms of mass units.

		Freundlich			Langmuir		
ACF adsorbent	Adsorbate	Log (K_F/[(mg/g)/(mg/L)^n])	n	R^2	q_m (mg/g)	Log (K_L/[L/g])	R^2
CACF	PHE	1.9	0.34	0.987	56	4.7	0.996
$CACFNH_2$	PHE	2.0	0.35	0.978	59	4.8	0.998
DeCACF	PHE	2.2	0.36	0.983	77	5.2	0.997
CACF	OCA	1.0	0.56	0.950	5.3	4.2	0.995
$CACFNH_2$	OCA	1.2	0.58	0.984	6.5	4.3	0.983
DeCACF	OCA	1.8	0.64	0.965	17	4.4	0.992

Figure 9S shows correlations between single point adsorption coefficients of PFOA, OCA and PHE with surface chemical properties of the corresponding ACFs.

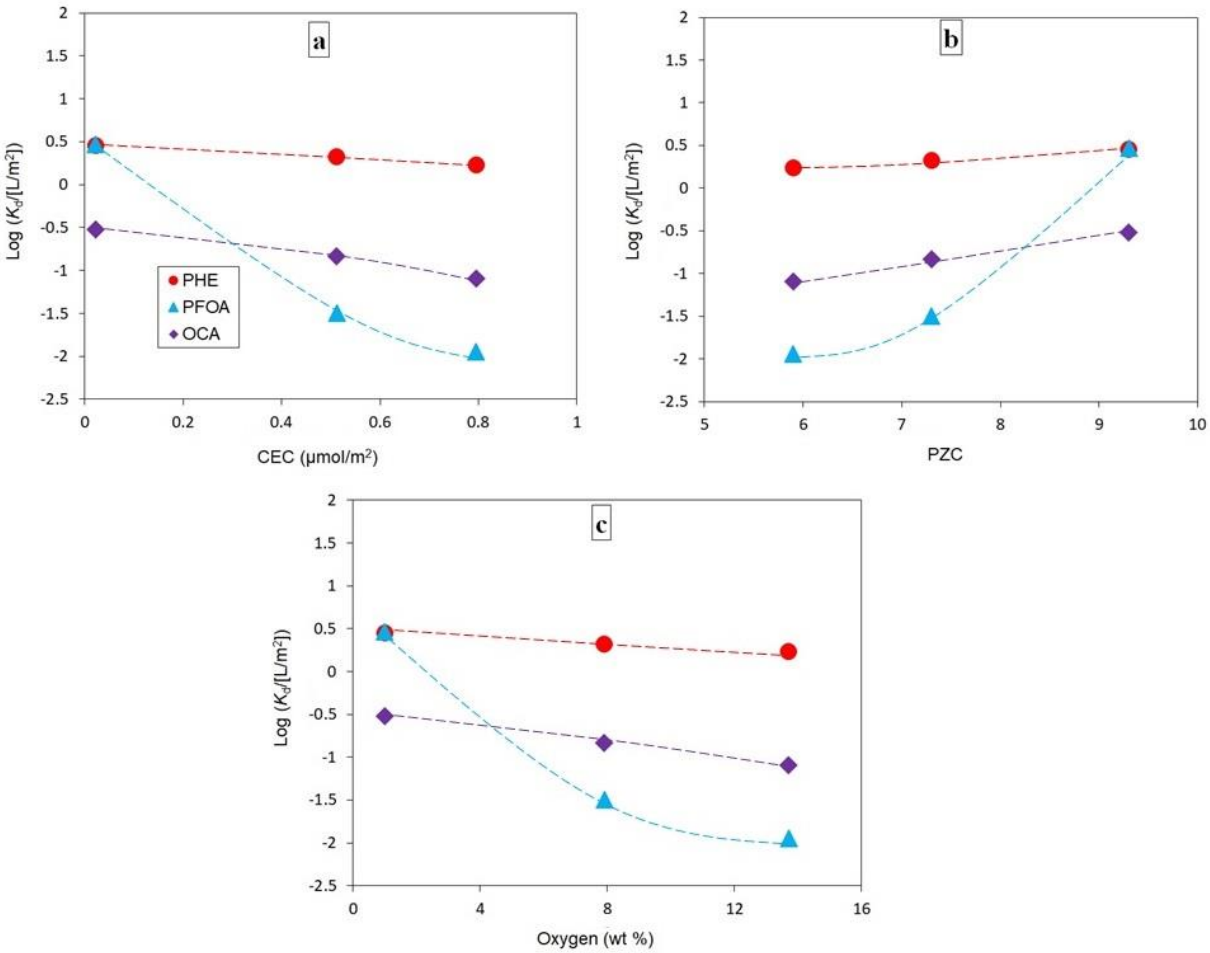

Figure 9S. Correlation between single point adsorption coefficients K_d and CEC (a), PZC (b) and oxygen content (c) of the ACFs in adsorption of PFOA, OCA and PHE from 10 mM Na_2SO_4 at pH 7. K_d values are obtained at $C_{e,\,PFOA}$ = 20 μg/L (0.048 μmol/L), $C_{e,\,PHE}$ = 10 μg/L (0.056 μmol/L) and $C_{e,\,OCA}$ = 10 μg/L (0.069 μmol/L). Lines were added as guide to the eye.

Effect of (in)organic ions on adsorption of PFOS and PFBA:

Figure 10S shows effect of inorganic ions on adsorption of PFOS and PFBA on the ACFs.

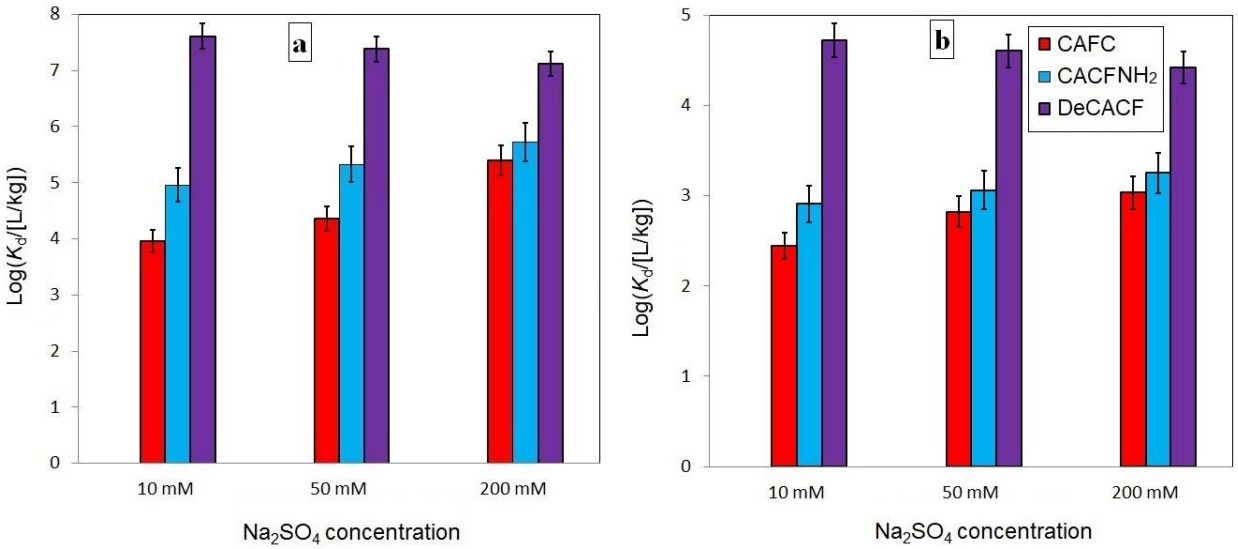

Figure 10S. Effect of inorganic ions on sorption of PFOS (a) and PFBA (b) on the ACFs. The experiments were carried out at pH 7 with C_0 = 1 mg/L PFOS or PFBA and adsorbent dosage 0.1 g/L for sorption of PFOS on all ACFs, 2 g/L for PFBA on CACF and $CACFNH_2$ and 0.5 g/L for PFBA on DeCACF. The maximum deviation of single values from the mean value of 3 experiments is reported as error bars.

Figure 11S illustrates effect of NOM on adsorption of PFOS and PFBA.

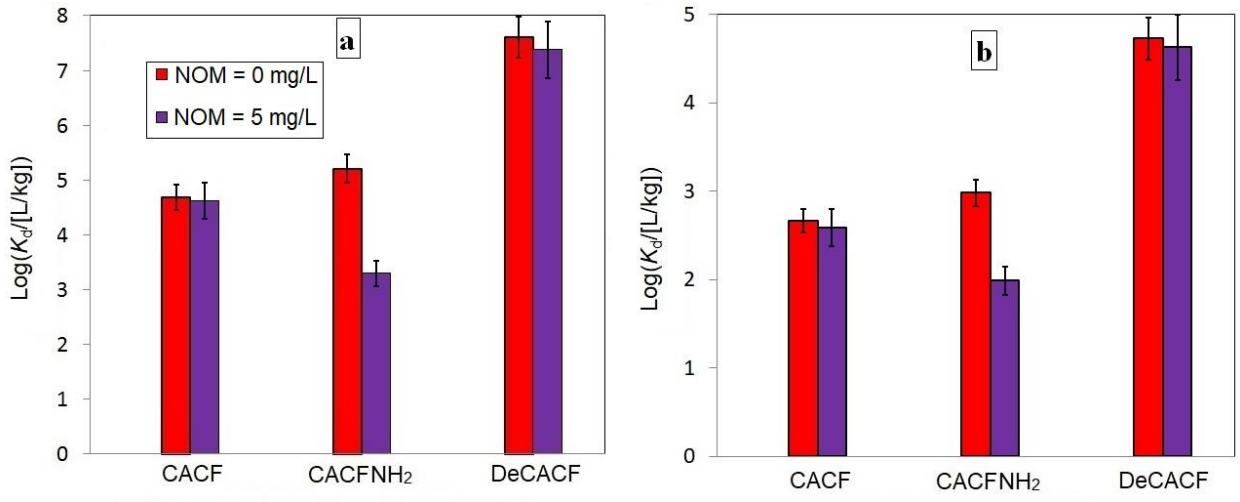

Figure 11S. Influence of NOM on sorption of PFOS (a) and PFBA (b) on the ACFs at pH 7. The experiments were performed at pH 7 with C_0 = 1 mg/L PFOS or PFBA in 10 mM Na_2SO_4 with and without NOM and adsorbent dosage 0.5 g/L CACF and $CACFNH_2$ and 0.1 g/L DeCACF for PFOS, 2 g/L CACF and $CACFNH_2$ and 0.5 g/L DeCACF for PFBA. The maximum deviation of single values from the mean value of the 3 experiments is reported as error bar.

Effect of pH on adsorption of PFOA, PFOS and PFBA:

Figure 12S shows adsorption of PFOA, PFOS and PFBA on the ACFs as a function of solution pH.

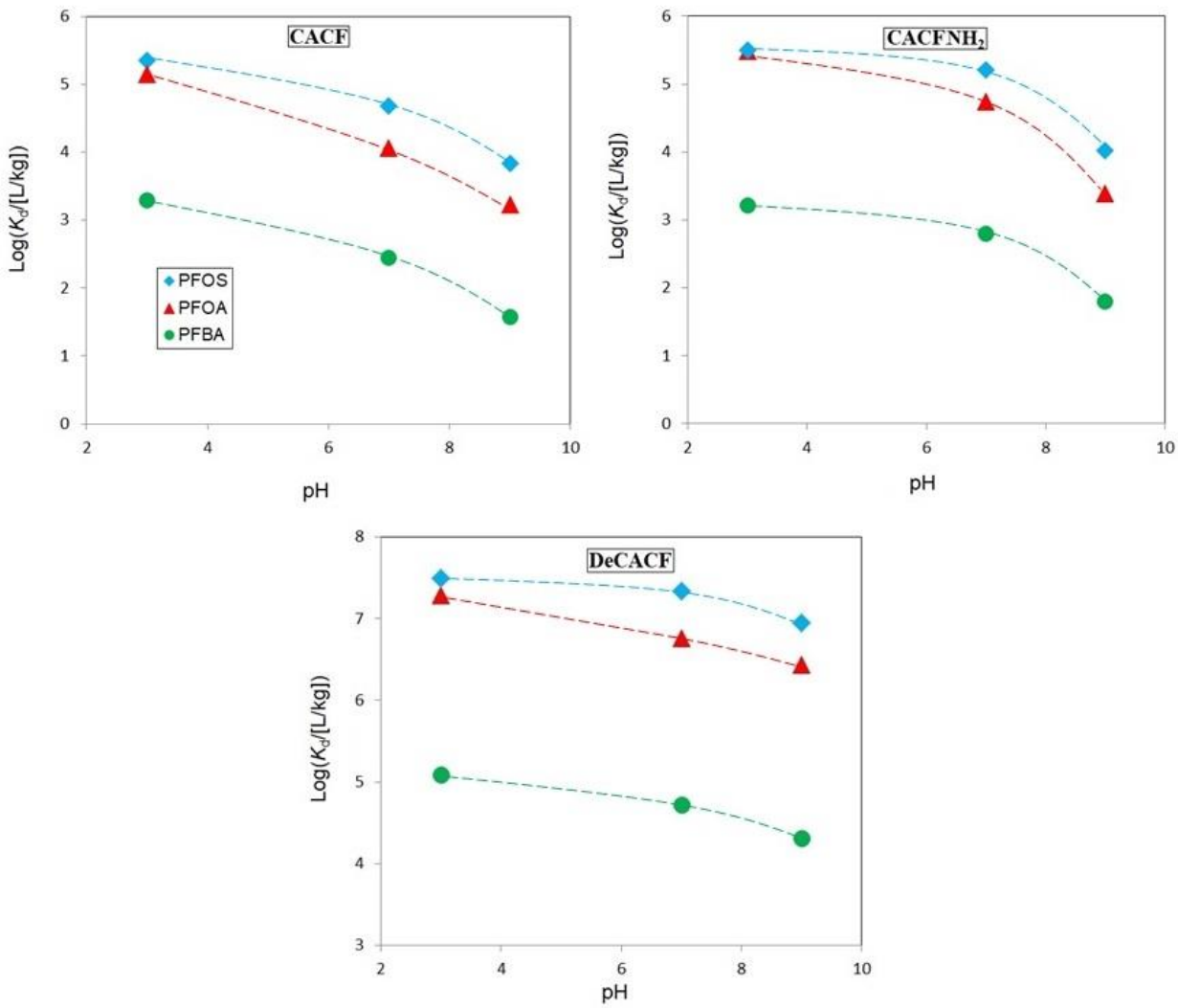

Figure 12S. Sorption of PFOA, PFOS and PFBA on DeCACF, CACF and $CACFNH_2$ at pH 3, pH 7 and pH 9. The experiments were performed with C_0 = 1 mg/L of adsorbate in 10 mM Na_2SO_4 and adsorbent dosage 0.02 g/L for DeCACF in uptake of PFOA and PFOS; 0.5 g/L for CACF and $CACFNH_2$ in sorption of PFOA and PFOS; 0.5 g/L for DeCACF in sorption of PFBA and 2 g/L for CACF and $CACFNH_2$ in uptake of PFBA. Lines were added as guide to the eye.

It is obvious that changing the pH influences more significantly adsorption of the PFAAs on CACF and $CACFNH_2$ than on DeCACF. The improvement in K_d for $CACFHN_2$ compared to CACF mainly holds for pH 7 where aminofunctionalisation leads to a reduced density of $–COO^-$ and

presence of $–NH_3^+$ groups. At pH 3 carboxylic groups are anyhow protonated and at pH 9 the positive charge of the amino groups is reduced. In contrast, defunctionalisation is beneficial for adsorption in the whole pH range. Also at pH 3, DeCACF is a better adsorbent than CACF even though at this pH repulsive charges due to carboxylate groups should be minimized. This highlights the importance of charge-compensating positive charges which were introduced by the defunctionalisation. These Lewis base sites are obviously only mildly affected by an increase in pH to 9 ($pK_a \geq 9$).

References

Ateia, M., Attia, M.F., Maroli, A., Tharayil, N., Alexis, F., Whitehead, D.C., Karanfil, T., 2018. Rapid removal of poly- and perfluorinated alkyl substances by poly(ethylenimine)-functionalized cellulose microcrystals at environmentally relevant conditions. Environmental Science & Technology Letters 5, 764-769.

Bandosz, T.J., Jagiello, J., Contescu, C., Schwarz, J.A., 1993. Characterization of the surfaces of activated carbons in terms of their acidity constant distributions. Carbon 31, 1193-1202.

Cai, N., Larese-Casanova, P., 2016. Application of positively-charged ethylenediamine-functionalized graphene for the sorption of anionic organic contaminants from water. Journal of Environmental Chemical Engineering 4, 2941-2951.

Gómez-Bombarelli, R., Calle, E., Casado, J., 2013. Mechanisms of lactone hydrolysis in neutral and alkaline conditions. J Org Chem 78, 6868-6879.

Hontoria-Lucas, C., López-Peinado, A.J., López-González, J.d.D., Rojas-Cervantes, M.L., Martín-Aranda, R.M., 1995. Study of oxygen-containing groups in a series of graphite oxides: physical and chemical characterization. Carbon 33, 1585-1592.

Keen, I., Broota, P., Rintoul, L., Fredericks, P., Trau, M., Grøndahl, L., 2006. Introducing amine functionalities on a Poly(3-hydroxybutyrate-co-3-hydroxyvalerate) surface: comparing the use of ammonia plasma treatment and ethylenediamine aminolysis. Biomacromolecules 7, 427-434.

Polovina, M., Babić, B., Kaluderović, B., Dekanski, A., 1997. Surface characterization of oxidized activated carbon cloth. Carbon 35, 1047-1052.

Saeidi, N., Kopinke, F.-D., Georgi, A., 2020. Understanding the effect of carbon surface chemistry on adsorption of perfluorinated alkyl substances. Chemical Engineering Journal 381, 122689.

Sörengård, M., Östblom, E., Köhler, S., Ahrens, L., 2020. Adsorption behavior of per- and polyfluoralkyl substances (PFASs) to 44 inorganic and organic sorbents and use of dyes as proxies for PFAS sorption. Journal of Environmental Chemical Engineering 8, 103744.

Zhang, D., He, Q., Wang, M., Zhang, W., Liang, Y., 2019. Sorption of perfluoroalkylated substances (PFASs) onto granular activated carbon and biochar. Environmental Technology, 1-12.

Zhang, Y., Zhi, Y., Liu, J., Ghoshal, S., 2018. Sorption of perfluoroalkyl acids to fresh and aged nanoscale zerovalent iron particles. Environmental Science & Technology 52, 6300-6308.